Prepared under Contract No. NAS 8-11036 Control No. TP-3-85373(IF)
June 25, 1964 CPB 02-1185-63

Not In

DEVELOPMENT OF AN ANALYTICAL TECHNIQUE FOR PREDICTING PROPERTIES OF COMPOSITE MATERIALS

Annual Summary Progress Report

July 1, 1963 to June 1, 1964

By
R. E. Silbernagel

Prepared For
George C. Marshall Space Flight Center
Huntsville, Alabama

CTL Missile/Space Technology Division
Studebaker Corporation
1240 Glendale-Milford Road
Cincinnati 15, Ohio

Prepared under Contract No. NAS 8-11036 Control No. TP-3-85373(IF)
June 25, 1964 CPB 02-1185-63

DEVELOPMENT OF AN ANALYTICAL TECHNIQUE FOR PREDICTING PROPERTIES OF COMPOSITE MATERIALS

Annual Summary Progress Report

July 1, 1963 to June 1, 1964

By
R. E. Silbernagel

Prepared For
George C. Marshall Space Flight Center
Huntsville, Alabama

CTL Missile/Space Technology Division
Studebaker Corporation
1240 Glendale-Milford Road
Cincinnati 15, Ohio

● STUDEBAKER'S MISSILE/SPACE TECHNOLOGY DIVISION
CINCINNATI, OHIO ● SANTA ANA, CALIFORNIA

FOREWORD

This report was prepared by CTL Missile/Space Technology Division of Studebaker Corporation, Cincinnati 15, Ohio, under Contract No. NAS 8-11036, Development of an Analytical Technique for Predicting Properties of Composite Materials, for the George C. Marshall Space Flight Center of the National Aeronautics and Space Administration. The work was administered under the technical direction of the Propulsion and Vehicle Engineering Laboratory, Materials Division of the George C. Marshall Space Flight Center with Mr. James E. Kingsbury acting as Project Manager.

This report covers the work conducted during the period of July 1, 1963, to June 1, 1964, and contains in narrative form a description of all technical findings to date. It contains a complete description of all principles and procedures involved, all testing procedures and modifications to these procedures, an evaluation of results obtained, conclusions and recommendations for future study made in connection with the work, and other such pertinent data as developed.

ABSTRACT

The work conducted under this contract and described in this report was demonstrative in nature and was based upon prior work performed at CTL during preliminary development of a procedure known as the Material Prediction Technique (MPT).

The work was performed specifically to demonstrate the validity of the parametric charting portion of the MPT. This was accomplished by testing composite materials in a selected hypothetical thermal environment which was a convective application.

In general, the development of this analytical technique was for the prediction of the physico-chemical, thermal, and other pertinent properties of composite materials. The technique was based upon the development of parametric charts in which the properties of various parent materials were correlated with the properties of composites made up of these various parent materials in various proportions.

Composite mats (batts, rovings, yarns and fabrics can also be made in this way) of pre-selected constituents were manufactured and test specimens fabricated. These specimens were tested to determine properties of the materials which are both dependent and independent of certain environmental conditions. When these first tests were completed, the parametric charts were developed. A second series of tests were performed and these confirmed the validity of the charting portion of the MPT.

Cross correlation of these charts was to be made to develop a composite in which each of the various parameters were to be optimized by varying the percentage composition of the various constituents and the processing history in accordance with the mode and composition predicted by the cross correlation. Such an optimized composite was to be processed and exposed to another selected hypothetical thermal environment to compare predicted performance with actual materials performance. However, due to the success of the charting technique it was decided to apply this cross correlation-optimization procedure to an actual thermal insulation such as found in the SATURN vehicle.

TABLE OF CONTENTS

LIST OF TABLES

LIST OF FIGURES

LIST OF FIGURES - Con't.

DEVELOPMENT OF AN ANALYTICAL TECHNIQUE FOR PREDICTING PROPERTIES OF COMPOSITE MATERIALS

SUMMARY

The work conducted under this contract and described in this report was demonstrative in nature and was based upon prior work performed at CTL during preliminary development of a procedure known as the Material Prediction Technique (MPT).

This work was performed specifically to demonstrate the validity of the parametric charting portion of the MPT. This was accomplished by testing composite materials in a selected hypothetical convective thermal environment.

In general, the development of this analytical technique was for the prediction of the physico-chemical, thermal, and other pertinent properties of composite materials. The technique was based upon the development of parametric charts in which the properties of various parent materials were correlated with the properties of composites made up of these various parent materials in various proportions.

Composite mats (batts, rovings, yarns and fabrics can also be made in this way) of pre-selected constituents were manufactured and test specimens fabricated. These specimens were tested to determine properties of the materials which are both dependent and independent of certain environmental conditions. When these first tests were completed, the parametric charts were developed. A second series of tests were performed and these confirmed the validity of the charting portion of the MPT. Cross correlation of these charts was to be made to develop a composite in which each of the various parameters were to be optimized by varying the percentage composition of the various constituents and the processing history in accordance with the mode and composition predicted by the cross correlation. Such an optimized composite was to be processed and exposed to another selected hypothetical thermal environment to compare predicted performance with actual materials performance. However, due to the success of the charting technique it was decided to apply this cross correlation-optimization procedure to an actual thermal insulation problem such as is found in the SATURN vehicle.

INTRODUCTION

In the constant search for materials to withstand the environment and operating conditions of space flight, such as is encountered during re-entry and in rocket motors, the practice has been to seek out new and exotic materials. At the same time this search for new and exotic materials continues at a rapid pace, there are currently available materials with known and proven properties which, if properly utilized, could be used to satisfy many of the present and future requirements.

CTL had been, for over a year before award of this contract, conducting studies directed toward the better utilization of present day materials and the expanded usage of some of the newer materials. The concept which resulted from these studies is known as the Material Prediction Technique (MPT) and preliminary tests conducted using this MPT tended to prove its feasibility.

In short, the MPT is an analytical method for selection of constituents and formulation of composite materials to satisfy specific operating and environmental conditions.

This is accomplished first by determining the operating and environmental conditions (such as time, heat pulse, enthalpy, pressure, velocity, etc.) then by establishing the critical conditions at specific locations on the article under consideration. When these performance parameters (physical envelope, weight limitations, area recession allowances, time-temperature profiles, etc.) are established, the major portion of the program is applied to a computer.

This is done in a manner which samples the effect of varying properties against these performance parameters so as to derive the idealized properties necessary for proper behavior of the part. Physical and thermal properties are examined in this way. A geometric analysis technique is then applied to ascertain the best mixture of fibers and resins to achieve the properties determined by the computer.

This procedure is employed for all selected specific locations on the part being analyzed. When the computer programs and geometric plotting of the parametric charts are completed, the results will show the optimum materials composition at all selected specific location on the part.

From this point on the MPT proceeds according to the steps outlined in the Summary of this report. It must be emphasized here and understood that the work described in this report was undertaken for one purpose only. This specific objective was to demonstrate the validity of the parametric charting portion of the MPT.

PROGRAM APPROACH

In order to accomplish the objective of this program economically and in the shortest time, CTL and NASA-GCMSFC personnel jointly selected three fibrous reinforcements for use with an organic binder material. Criteria employed in the selection of these materials from a number of candidates were: (A) the known physical and thermal characteristics of these state of the art materials, (B) the ready availability of these materials, and (C) the capability of being processed on standard equipment according to standard manufacturing and fabrication methods.

The three fibrous reinforcements chosen were chrysotile asbestos, "E" glass and graphite. The organic binder selected for use with these fibers was CTL-91LD phenolic resin. These four materials exhibited a wide range in the property values which were investigated under this program. It must be emphasized that this selection was purely arbitrary and in no way limits use of other fibers.

Subsequent to this material selection, CTL procured Canadian Cassiar grade chrysotile asbestos fibers 1" and 2" in length; J. P. Stevens Co., Inc. "E" glass fibers 1/4" to 1/2" in length; and National Carbon Co. WFA graphite fibers 1/4" to 1/2" in length. Non-woven mats were processed according to the following theoretical schedule:

Mat No.	Primary Fiber (85.8%)	Secondary Fibers (7.1% each)
1	Asbestos	Glass & Graphite
2	Glass	Graphite & Asbestos
3	Graphite	Asbestos & Glass

The production of these initial experimental fiber mats was accomplished on standard Proctor textile processing machinery. A complete description of this equipment and the manufacturing procedures used is provided in Appendix 1, Procedures for Manufacturing Non-Woven Fibrous Mats. The resultant mats were approximately 50 feet in length x 25 inches in width, ranged from .020 to .040 inches in thickness, and weighed from 1 to 1-1/2 ounces per square foot. There is no limit to length of rolls using this process.

These first experimentally produced non-woven mats were generally non-uniform and of poor construction. However, Mat No. 1 was noticeably better than Mat Nos. 2 and 3. The difference was attributed to the fact that the greater length of the asbestos fibers, which were well opened and exhibited better carrying ability, overcame the short fiber lengths of the graphite and glass thereby resulting in better arrangement during processing.

Impregnation of the three mat compositions was achieved by using standard vacuuming techniques. The CTL-91LD phenolic resin was "B" staged, in a circulating air oven at 250°F, so as to yield final molded composite test panels having the theoretical target resin contents of 30% and 50%. These panels would be tested and provide the data needed for the initial

step in chart construction and development.

All test panels were press molded at pressures ranging from 300 to 1,000 psi and were cured for 2 hours at 280° to 310°F. The test panels which were targeted for 30% resin content were designated by adding A to the Mat No. and those targeted for 50% resin content were designated by adding B to the Mat No. For example, test panel 1A would indicate a 30% resin content panel having asbestos as the primary reinforcing fiber with glass and graphite as the secondary fibers. 3B would indicate graphite was the primary reinforcing fiber with glass and asbestos as the secondary fibers in a test panel having 50% resin content.

The final molded test panels were 20" x 13" x 1/2". These were sectioned to obtain sufficient test specimens of the required shapes and sizes indicated in the sampling plan shown in Figure No. 1.

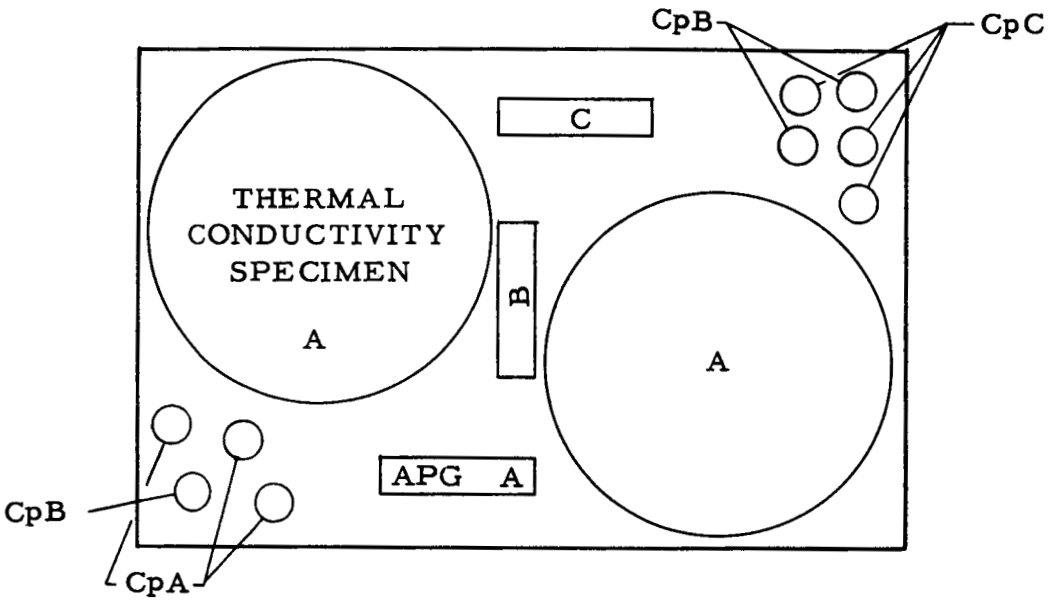

FIGURE NO. 1 TEST SPECIMEN LOCATIONS IN TEST PANELS

Three tests, to establish some reliability of data, per test panel type per property were conducted in order to provide enough information to construct parametric charts. The materials properties which were selected by CTL and NASA-GCMSFC personnel for experimental determination in this program were as follows:

1) Density (specific gravity).
2) Specific heat @ 500°F.
3) Thermal Conductivity @ 500°F.
4) Melting Point.
5) Emissivity.
6) Effective heat of ablation.
7) Mass loss rate.
8) Effective thermal conductivity.

The methods which were followed in the determination of these properties are described in detail in Appendix 2, Testing Procedures and Equipment.

TABLE 1

SHORT FIBER COMPOSITES AND THEIR PROPERTIES

A. Calculated Constituent Percentages

Composite No.	%91LD Resin	% Asbestos	% "E" Glass	% Graphite
1A	40	51.4	4.3	4.3
1B	50	42.8	3.6	3.6
2A	35	4.6	55.8	4.6
2B	50	3.6	42.8	3.6
3A	35	4.6	4.6	55.8
3B	52.1	3.4	3.4	41.1

B. Composite Properties

Composite No.	Density (lbs/ft^3)	Specific Heat @ 500°F. (BTU/lb.°F.)	Thermal Conductivity @ 500°F. (BTU/hr.ft°F.)	Melting Point (° F.)	Effective Heat of Ablation (BTU/lb.)	Mass Loss Rate ($lbs/ft^2 sec.$)	Effective Thermal Conductivity (BTU/ft.hr.°F.)
1A	97.9	.196	.228	2455	5,450	.0156	.943
1B	86.3	.330	.196	2420	6,510	.0129	.948
2A	91.6	.232	.332	2015	5,310	.0192	.942
2B	85.0	.221	.218	1940	6,110	.0162	.943
3A	87.8	.166	.438	6500	19,250	.0062	1.001
3B	89.1	.360	.340	6400	16,750	.0071	1.104
Virgin Materials:							
91LD	71.7	.48	.216	-	-	-	-
Asbestos	146.8	.29	-	2565	-	-	-
"E" Glass	154.5	.22	-	1880	-	-	-
Graphite	97.6	.42	-	6600	-	-	-

STUDEBAKER'S MISSILE/SPACE TECHNOLOGY DIVISION
CINCINNATI, OHIO • SANTA ANA, CALIFORNIA

The properties determinations on these materials resulted in the data tabulated in Table 1. All property values determined from arc plasma generator (APG) tests in this program were obtained by using the channel flow test technique (Figure No. 2). The test material formed the long wall of the tunnel whereas a cold wall calorimeter formed the short wall of the tunnel.

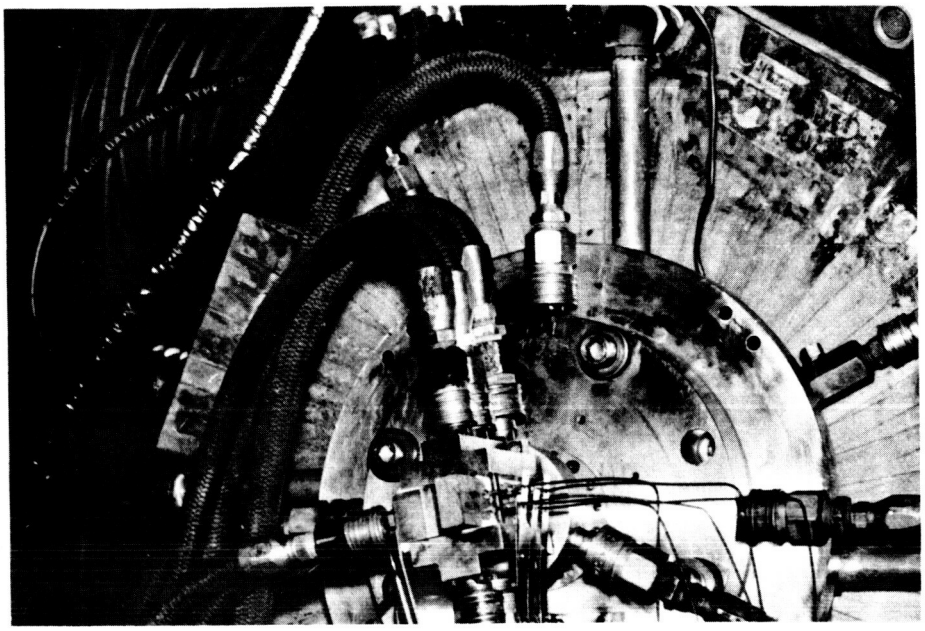

FIGURE NO. 2 CHANNEL FLOW TEST TECHNIQUE

The pre-selected (by joint agreement between NASA-GCMSFC & CTL personnel) hypothetical convective thermal environment called for all APG tests to be conducted at a heat flux rate of from 75 to 100 BTU/ft^{2}sec.; the test gas was to be a mixture of 80% nitrogen and 20% oxygen; the chamber pressure was to be from 1 to 2 atmospheres; and the test exposure duration was to be from 1 to 3 minutes.

Unfortunately, in this first series of tests the data on effective heat of ablation, mass loss rate, and effective thermal conductivity (which was obtained simultaneously during each APG test specimen run) was not obtained at the pre-selected, low heat flux test condition. As much oxygen as possible was added downstream of the arc, during these tests, in an effort to reduce the heat flux to the desired range, keep the enthalpy low and increase the chamber pressure as much as possible. Yet, these first tests actually were conducted at 139 BTU/ft^2 sec. and 17.5 psi. chamber pressure. This was the lowest heat rate possible, at the time, which would maintain the arc in the APG. The low power setting caused wide ranging in the gas temperature, enthalpy, etc., as indicated by the visicorder data traces.

Modifications were made to the APG facility to insure greater efficiency and maintain the arc at lower power inputs. Better visicorder traces were obtained and a fine degree of accuracy in the accumulated data was provided.

TABLE 2

SHORT FIBER COMPOSITES AND THEIR PROPERTIES

(Repeat rests at different APG conditions)

A. Calculated Constituent Percentages

Composite No.	% 91LD Resin	% Asbestos	% "E" Glass	% Graphite
1A	40	51.4	4.3	4.3
1B	50	42.8	3.6	3.6
2A	35	4.6	55.8	4.6
2B	50	3.6	42.8	3.6
3A	35	4.6	4.6	55.8
3B	52.1	3.4	3.4	41.1

B. Composite Properties

Composite No.	Density (lbs/ft^3)	Specific Heat @ 500°F. (BTU/lb. °F.)	Thermal Conductivity @ 500°F. (BTU/hr.ft°F.)	Melting Point (°F.)	Emissivity	Effective Heat of Ablation (BTU/lb.)	Mass Loss Rate ($lbs/ft^2sec.$)	Effective Thermal Conductivity (BTU/ft.hr. °F.
1A	97.9	.196	.228	2455	.823	13,515	.0059	.718
1B	86.3	.330	.196	2420	.907	11,334	.0069	.710
2A	91.6	.232	.332	2015	.750	6,390	.0119	.769
2B	85.0	.221	.218	1940	.900	9,002	.0085	.733
3A	87.8	.166	.438	6500	.970	21,531	.0035	.876
3B	89.1	.360	.340	6400	.979	16,983	.0045	.791
Virgin Materials:								
91LD	71.7	.48	.216	-	-	-	-	-
Asbestos	146.8	.29	-	2565	-	-	-	-
"E" Glass	154.5	.22	-	1880	-	-	-	-
Graphite	97.6	.42	-	6600	-	-	-	-

TABLE 3

EFFECTIVE HEAT OF ABLATION TEST DATA

Composite No.	Cold Wall Heat Rate $\left(\frac{BTU}{ft^2\ sec.}\right)$	Power Input $\left(\frac{BTU}{sec.}\right)$	H_2O Mass Flow (lbs/sec.)	H_2O Temp. Increase (°F)	Hot Wall Temp. (°F)	Hot Wall Enthalpy (BTU/lb.)	Mass Flow (lbs/sec.)	Recession Rate (ft./sec.)	Density (lbs/ft^3)	Eff. Heat of Ablation (BTU/lb.)
1A	94	300	22.4	11.3	2295	719.28	.01005	.00006	97.9	13,515
1B	94	292	22.2	11.09	2490	776.05	.00992	.00008	86.3	11,334
2A	94	299	21.5	12.02	2425	757.07	.01016	.00013	91.6	6,390
2B	94	302	21.6	12.02	2465	768.75	.01012	.00010	85.0	9,002
3A	94	277	21.6	11.18	2155	678.81	.0102	.00004	87.8	21,531
3B	94	298	21.8	11.74	2330	729.42	.0112	..00005	89.1	16,983

Remarks

1) Test gas was 80% Nitrogen with 20% Oxygen injected downstream of the arc.
2) Hot wall gas enthalpy values were obtained from Table 7, Thermodynamic Properties of Dry Air, Aircraft and Missile Propulsion, Volume I, M. J. Zucrow, John Wiley & Sons, Inc., 1958.

Sample Calculation:

$$Heff = \frac{qo}{M} = \frac{qcw\left[\frac{He-Hw}{He}\right]}{\rho_b\, Vw} = \frac{qcw\left[\frac{\frac{P-L}{\dot{m}g}-Hw}{\frac{P-L}{\dot{m}g}}\right]}{\rho_b\, Vw} = \frac{qcw\left[\frac{\frac{P-(\dot{m}wCp\Delta t)}{\dot{m}g}-Hw}{\frac{P-(\dot{m}wCpw\Delta t)}{\dot{m}g}}\right]}{\rho_b\, Vw}$$

Composite No. 1A:

$$Heff = \frac{94\left[\frac{\frac{300-(22.4 \times 11.3)}{.01005}-719.28}{\frac{300-(22.4 \times 11.3)}{.01005}}\right]}{97.9 \times .00006} = \frac{94\left[\frac{4622-719.28}{4622}\right]}{.00587} = \frac{94\left[\frac{3902.72}{4622}\right]}{.00587} = 94\ \frac{(.844)}{.00587} =$$

$$Heff = \frac{79.336}{.00587} = 13,515$$

TABLE 4
MASS LOSS RATE TEST DATA

Composite No.	Density (lbs/ft^3)	Exposure Duration (seconds)	Spec. Wt. Before Firing (grams)	Total Mass Loss (grams)	Total Mass Loss (%)	Total Ablation (inches)	Recession Rate (in./sec.)	Mass Loss Rate ($lbs./ft^2sec$)
1A	97.9	90	57.0605	7.305	12.8	.068	.00075	.0059
1B	86.3	90	46.8848	9.0838	19.4	.083	.00092	.0069
2A	91.6	90	45.0942	8.0601	14.0	.137	.00152	.0119
2B	85.0	90	40.4571	9.9772	24.6	.111	.00123	.0085
3A	87.8	90	47.4085	8.1234	17.1	.049	.00054	.0035
3B	89.1	90	47.8151	10.2939	21.5	.056	.00062	.0045

Sample Calculation: $MLR = \frac{lbs.}{ft^2sec.} = \frac{lbs.}{ft^3} \times \frac{ft}{sec.}$ or Density x Recession Rate

Composite No. 1A: $MLR = 97.9 \times .00006 = .0059$

STUDEBAKER'S MISSILE/SPACE TECHNOLOGY DIVISION
CINCINNATI, OHIO • SANTA ANA, CALIFORNIA

TABLE 5

EFFECTIVE THERMAL CONDUCTIVITY TEST DATA

Composite No.	Chamber Pressure (psi)	Gas Enthalpy (BTU/lb.)	Gas* Temp. (°F)	Hot Wall Heat Rate (BTU/ft²sec.)	Temp. °F@TC Location after 30 seconds				Gas Temp. minus TC Temp. in °F				Keff@TC Location (BTU/ft.hr.°F)	Keff Average (BTU/ft.hr.°F)
					TC#1 (.4" Deep)	TC#2 (.3" Deep)	TC#3 (.2" Deep)	TC#4 (.1" Deep)	TC#1 (.4" Deep)	TC#2 (.3" Deep)	TC#3 (.2" Deep)	TC#4 (.1" Deep)		
1A	18.2	4622	8707	79.336	75	104	130	621	8632	8603	8577	8086	#1) 1.129	
													#2) .845	.718
													#3) .574	
													#4) .324	
1B	18.3	4615	8648	78.208	75	98	144	322	8573	8550	8504	8326	#1) 1.123	
													#2) .842	.710
													#3) .566	
													#4) .310	
2A	18.7	3958	7897	76.046	118	177	235	847	7779	7720	7662	7050	#1) 1.195	
													#2) .920	.769
													#3) .611	
													#4) .350	
2B	18.6	4133	8300	76.516	75	235	235	827	8225	8065	8065	7473	#1) 1.144	
													#2) .868	.733
													#3) .584	
													#4) .335	
3A	18.3	3463	6940	75.576	177	308	496	738	6763	6632	6444	6202	#1) 1.364	
													#2) 1.033	.876
													#3) .712	
													#4) .394	
3B	18.3	3727	7570	75.576	118	130	321	643	7452	7440	7249	6927	#1) 1.226	
													#2) .925	.791
													#3) .642	
													#4) .360	

*Obtained from NACA TN4265, Composition & Thermodynamic Properties of Air in Chemical Equilibrium, W. E. Moeckel and Kenneth C. Weston, Lewis Flight Propulsion Laboratory, Cleveland, Ohio, April, 1958.

Sample Calculations: $Keff = \frac{BTU}{ft\ hr\ ^oF} = \frac{BTU}{ft^2 sec} \times \frac{ft}{^oF} = \frac{qo}{\Delta t} \times \frac{TC\ depth}{12} \times 3600$

Composite No. 1A:

$$\#1\text{-Keff} = \frac{79.336}{8632} \times .409 \times 300 = 1.129$$

$$\#2\text{-Keff} = \frac{79.336}{8603} \times .306 \times 300 = .845$$

$$\#3\text{-Keff} = \frac{79.336}{8577} \times .207 \times 300 = .574$$

$$\#4\text{-Keff} \quad \frac{79.336}{8086} \times .110 \times 300 = .324$$

Average Keff .718

APG Test Specimen Sketch:

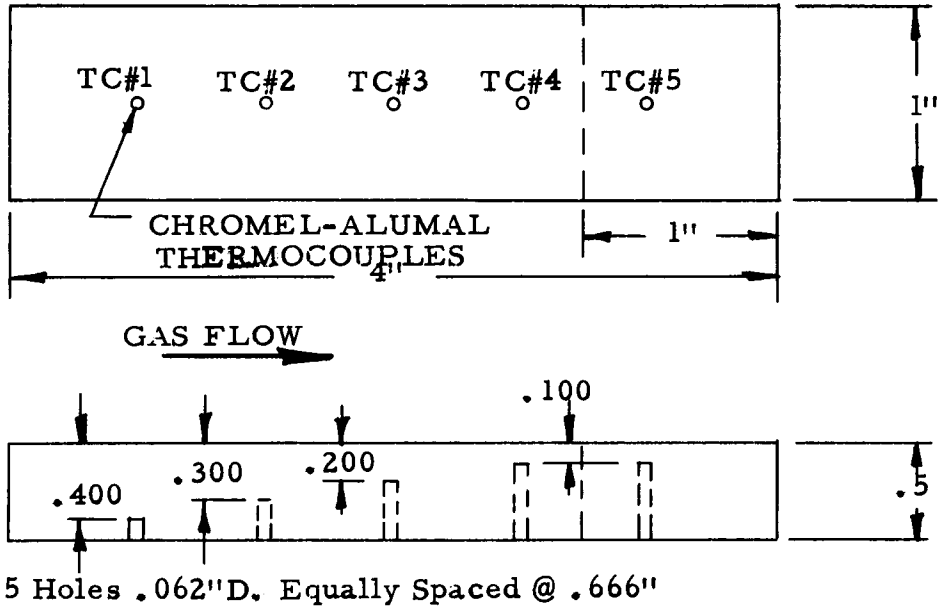

A second series of tests was performed on the same materials and this data is listed in Table 2. These tests were conducted within the preselected convective thermal environment originally specified. Supporting data and information describing methods used to obtain these values is supplied in Tables 3, 4 and 5.

Concurrently with the property determinations and as data became available, parametric charts were prepared for each of the properties determined on the previously selected, impregnated composites designated as 1A through 3B. Examination of this data and the resultant plotted charts revealed a scatter of the average test values producing quite a bit of surface contour irregularity for three of the properties determined. These three properties were specific heat, thermal conductivity and the mass-loss rate. Generally, the parametric charts (Figure Nos. 3 through 10) for density, melting point, emissivity, effective heat of ablation, and effective thermal conductivity demonstrated that there was good to excellent agreement between the empirical data and predicted values which would be obtained by employing the parametric charting technique.

For the reasons cited in the Discussion of Results section of this report, the initially selected fiber mat compositions were repeated using 2" to 3" length graphite and glass fibers. These mats as typified by Figure No. 20 were an improvement over the initial mats produced with the shorter fibers. Impregnation of these mats, fabrication of test panels and preparation of test specimens was accomplished by using the same procedures employed with the short fiber composites.

Testing of these long fiber composites was conducted in the same manner as before with three exceptions. These three exceptions to the Testing Procedures listed in Appendix 2 were as follows:

(a) Method 2 was used to determine the melting points of the APG specimens; on
(b) only the actual time that mass loss was experienced, as determined by Method 2, was used in the calculation of mass loss rate. This was done rather than assume that mass loss was experienced over the entire specimen exposure time;
(c) thermocouple orientation and depths were changed from those indicated in the sketch on Table 5 to those depicted in the sketch on Table 9. This was done to provide better correlation of time-temperature profile data and yield more accurate calculation of thermal conductivity data.

The data on this series of tests is listed in Table 6 with supporting data and descriptive information supplied in Tables 7, 8 and 9.

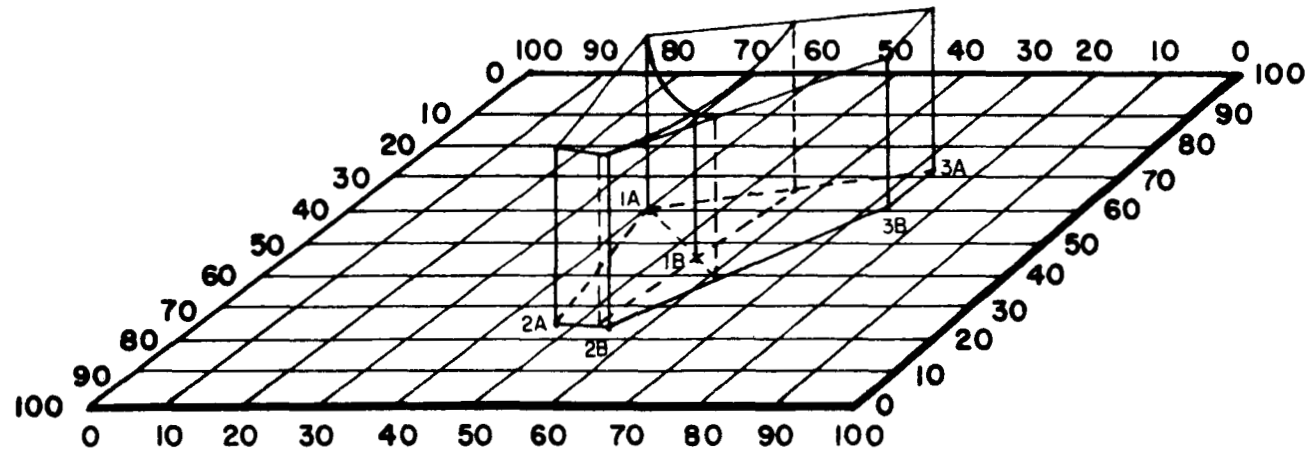

FIGURE NO. 3 PARAMETRIC CHART FOR DENSITY

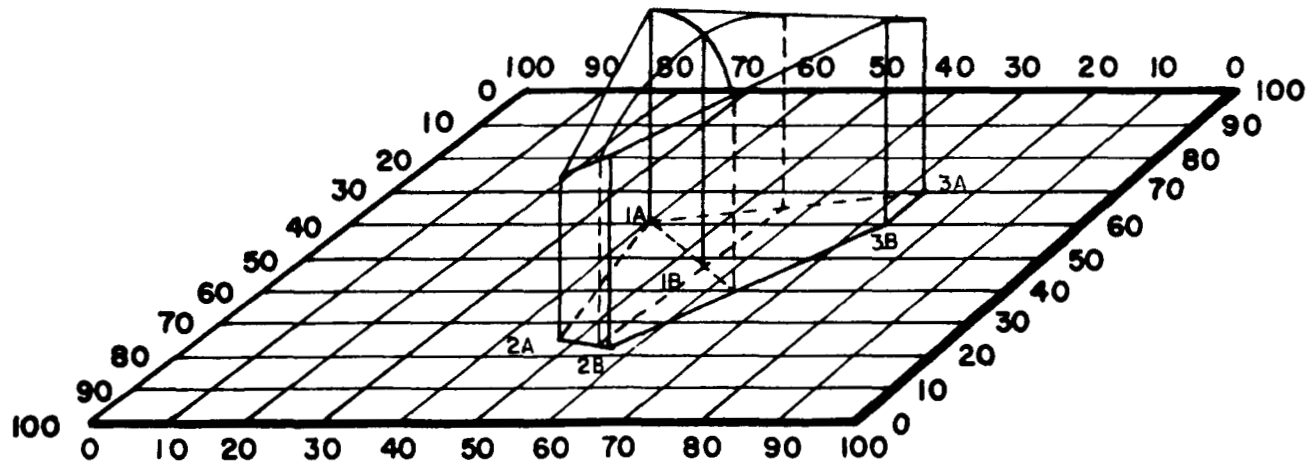

FIGURE NO. 4 PARAMETRIC CHART FOR SPECIFIC HEAT

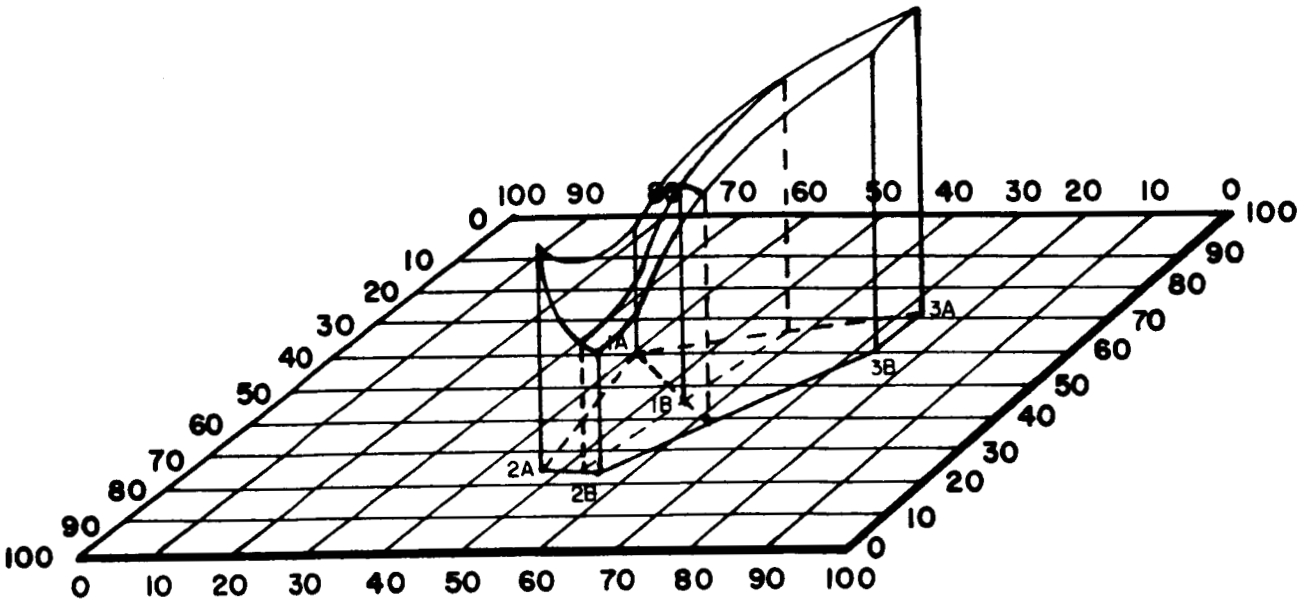

FIGURE NO. 5 PARAMETRIC CHART FOR THERMAL CONDUCTIVITY

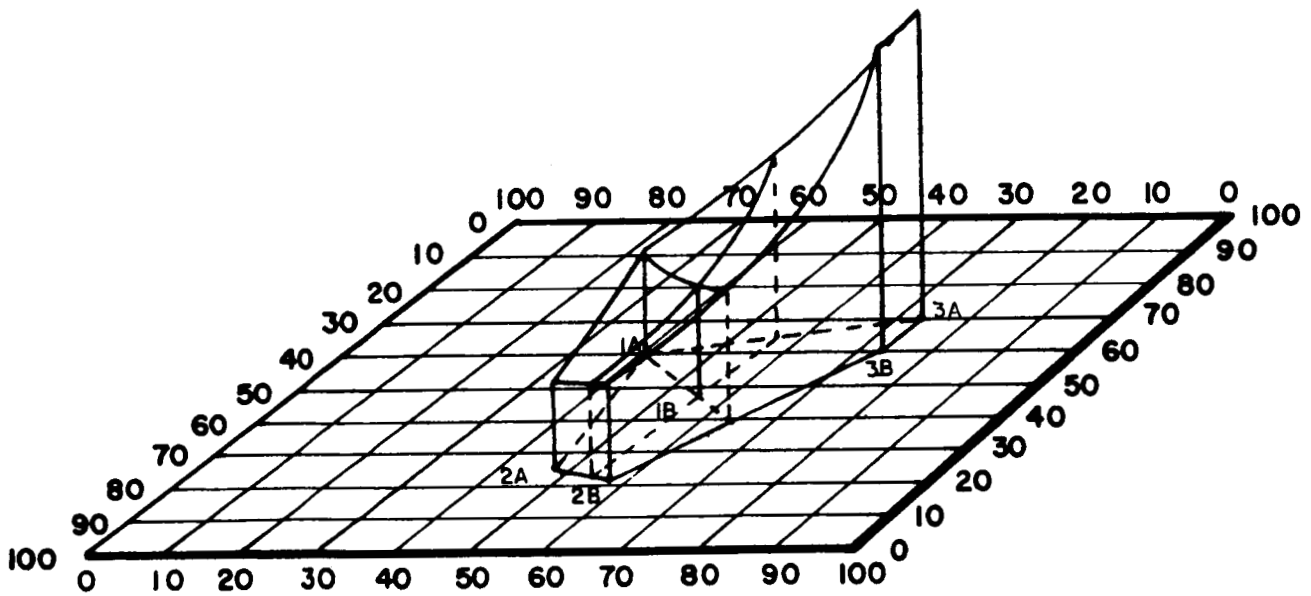

FIGURE NO. 6 PARAMETRIC CHART FOR MELTING POINT

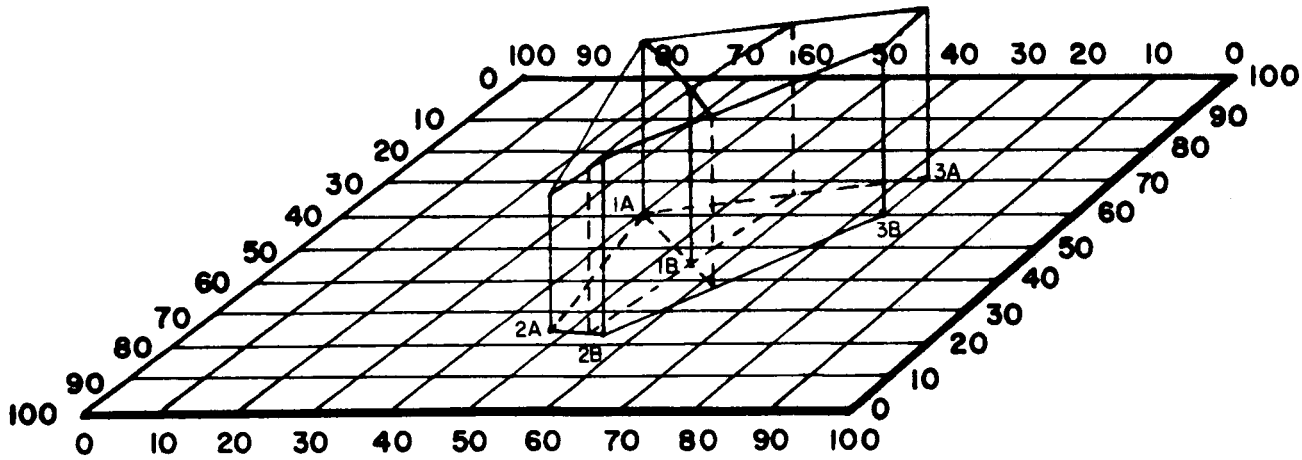

FIGURE NO. 7 PARAMETRIC CHART FOR EMISSIVITY

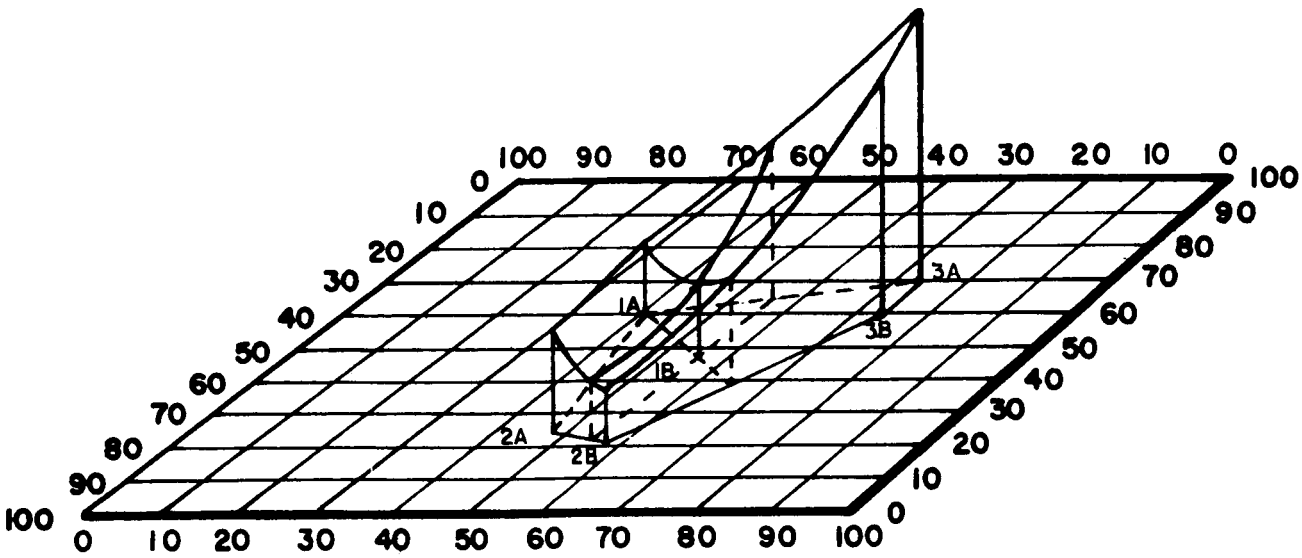

FIGURE NO. 8 PARAMETRIC CHART FOR EFFECTIVE HEAT OF ABLATION

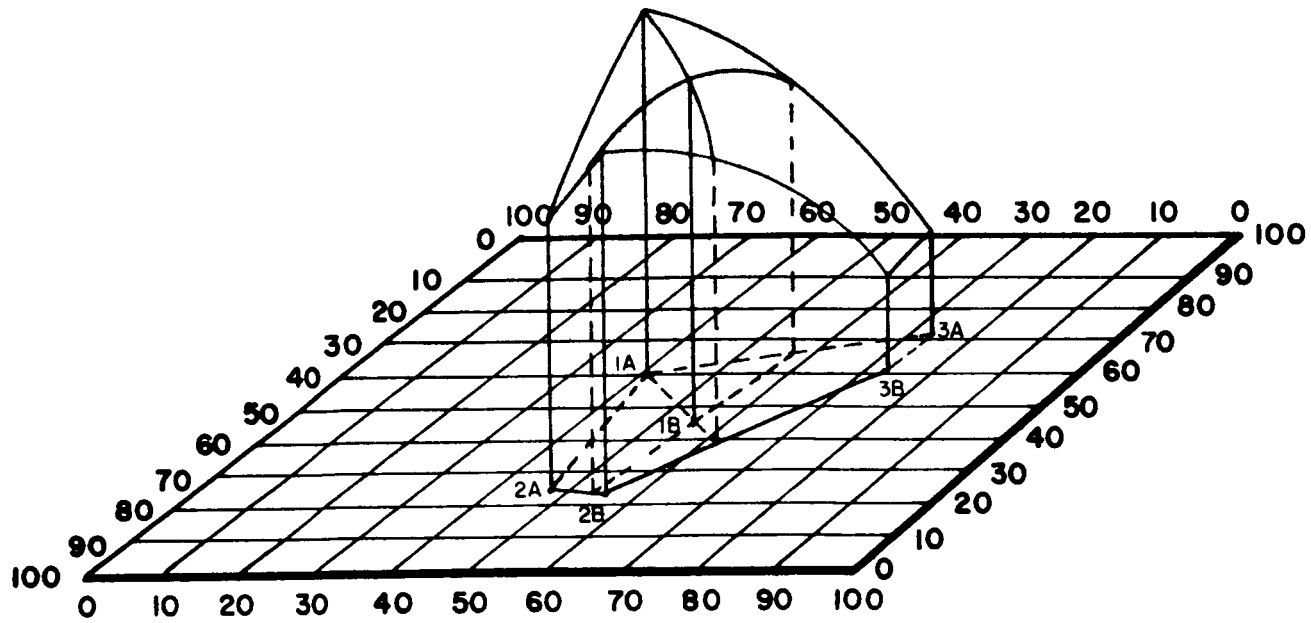

FIGURE NO. 9 PARAMETRIC CHART FOR MASS LOSS RATE

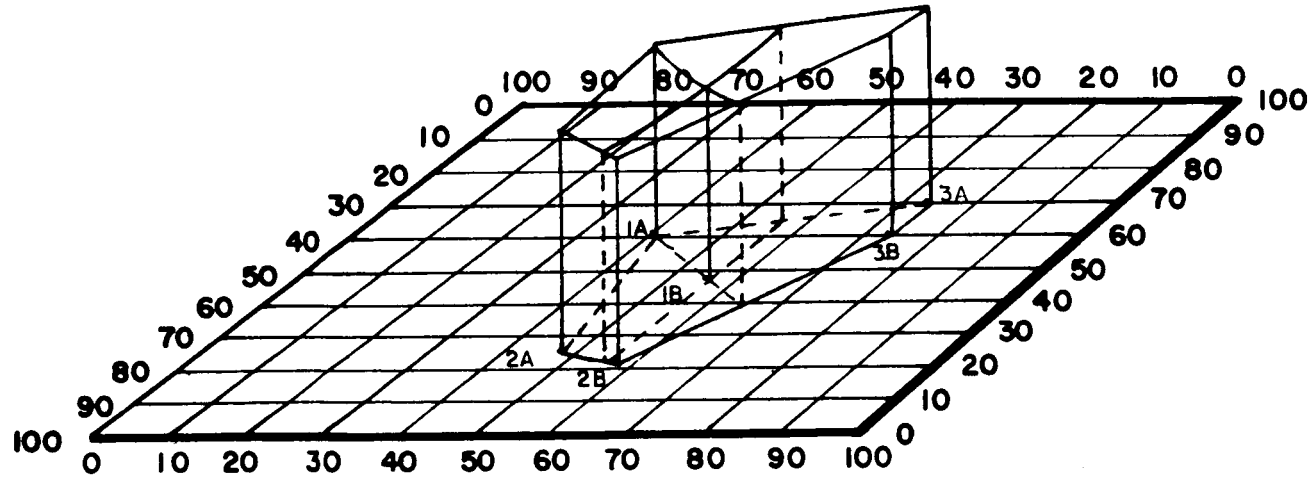

FIGURE NO. 10 PARAMETRIC CHART FOR EFFECTIVE THERMAL CONDUCTIVITY

TABLE 6

LONG FIBER COMPOSITES AND THEIR PROPERTIES

A. Constituent Percentages by Actual Analyses

Composite No.	% 91LD Resin	% Asbestos	% "E" Glass	% Graphite
1A	26.53	67.00	5.20	1.27
1B	47.93	47.05	4.00	1.02
2A	38.04	10.81	47.85	3.30
2B	43.07	8.89	44.78	3.26
3A	46.81	3.06	2.69	47.44
3B	54.44	2.11	2.17	41.28

B. Composite Properties

Composite No.	Density (Lbs/ft^3)	Specific Heat @ 500°F. (BTU/lb.°F.)	Thermal Conductivity @ 500°F. (BTU/hr.Ft°F.)	Melting Point (°F.)	Emissivity	Effective Heat of Ablation (BTU/lb.)	Mass Loss Rate (lbs/ft^{2}sec.)	Effective Thermal Conductivity BTU/ft.hr.°F.
1A	89.4	.344	.136	2260	.936	3,691	.0188	1.016
1B	78.6	.358	.232	2255	.923	4,016	.0181	1.006
2A	90.7	.258	.244	1945	.686	5,342	.0141	1.122
2B	78.7	.305	.122	2140	.907	3,431	.0177	1.050
3A	83.5	.272	.326	-	.917	14,428	.0049	1.106
3B	80.4	.319	.310	-	.961	11.531	.0055	1.068
Virgin Materials:								
91LD	71.7	.352	.216	-	-	-	-	-
Asbestos	146.8	.246	-	2565	-	-	-	-
"E" Glass	154.5	.151	-	1880	-	-	-	-
Graphite	97.6	.234	-	6600	-	-	-	-

TABLE 7

EFFECTIVE HEAT OF ABLATION TEST DATA

Composite No.	Cold Wall Heat Rate $\left(\frac{BTU}{ft^2\ sec.}\right)$	Power Input $\left(\frac{BTU}{sec.}\right)$	H_2O Mass Flow $\left(\frac{lbs}{sec.}\right)$	H_2O Temp Increase (°F)	Hot Wall Temp. (°F.)	Hot Wall Enthalpy $\left(\frac{BTU}{lb.}\right)$	Mass Flow $\left(\frac{lbs}{sec}\right)$	Recession Rate $\left(\frac{ft}{sec.}\right)$	Density $\left(\frac{lbs.}{ft^3}\right)$	Eff. Heat of Ablation (BTU/lb)
1A	95	371	26.6	12.82	2260	709.14	.0120	.00021	89.4	3,691
1B	95	365	26.5	12.46	2255	707.69	.0121	.00023	78.6	4,016
2A	95	363	25.9	12.73	1890	617.25	.0121	.00016	90.7	5,342
2B	95	363	26.4	12.82	2140	674.49	.0120	.00022	78.7	3,431
3A	95	356	25.9	12.47	2340	732.33	.0119	.000059	83.5	14,428
3B	95	356	25.7	12.61	2490	776.05	.0120	.000074	80.4	11,531

Remarks:

1) Test gas was 80% Nitrogen with 20% Oxygen injected downstream of the arc.

2) Hot wall gas enthalpy values were obtained from Table 7, Thermodynamic Properties of Dry Air, Aircraft and Missile Propulsion, Volume I, M. J. Zucrow, John Wiley & Sons, Inc. 1958.

3) Actual time that mass loss was experienced, as determined from movie film of the test run, was employed.

4) Calculated in same way as shown in Table 3.

TABLE 8

MASS LOSS RATE TEST DATA

Composite No.	Density (lbs/ft^3)	Exposure Duration (seconds)	Spec. Wt. Before Firing (grams)	Total Mass Loss (grams)	Total Mass Loss (%)	Total Ablation (inches)	Recession Rate (in/sec.)	Mass Loss Rate ($lbs/ft^2sec.$)
1A	89.4	80.1	46.4353	9.4167	20.3	.206	.0025	.0188
1B	78.6	79.6	41.9091	9.9037	23.6	.219	.0027	.0181
2A	90.7	84.7	50.3549	5.0397	10.0	.154	.0018	.0141
2B	78.7	85.7	41.4980	11.3006	27.2	.229	.0026	.0177
3A	83.5	90	44.6414	8.9151	20.0	.064	.00071	.0049
3B	80.4	90	41.3011	14.2945	30.2	.080	.0009	.0055

Remarks:

1) Actual time that mass loss was experienced, as determined from movie films of the test runs, was employed.

2) Calculated in same way as shown in Table 4.

TABLE 9

EFFECTIVE THERMAL CONDUCTIVITY TEST DATA

Composite No.	Chamber Pressure (psi)	Gas Enthalpy (BTU/lb.)	Gas* Temp. (°F)	Hot Wall Heat Rate (BTU/ft²sec.)	Temp. °F@TC Location after 30 seconds				Gas Temp. minus TC Temp. in °F				Keff@TC Location (BTU/ft hr °F)	Keff Average (BTU/ft hr °F)
					TC#1 (.3" Deep)	TC#2 (.3" Deep)	TC#3 (.3" Deep)	TC#4 (.1" Deep)	TC#1 (.3" Deep)	TC#2 (.3" Deep)	TC#3 (.3" Deep)	TC#4 (.1" Deep)		
1A	20.0	2499	5892	63.23	145	147	109	889	5747	5745	5783	5003	#1) 1.019 #2) 1.019 #3) 1.010 #4) .403	1.016
1B	19.8	3024	6467	69.11	114	138	109	805	6353	6329	6358	5662	#1) 1.002 #2) 1.016 #3) 1.001 #4) .388	1.006
2A	19.9	2700	6107	72.10	233	263	155	943	5874	5844	5952	5164	#1) 1.125 #2) 1.131 #3) 1.109 #4) .438	1.122
2B	20.0	2087	5376	59.87	140	136	145	1140	5236	5240	5231	4236	#1) 1.050 #2) 1.049 #3) 1.052 #4) .442	1.050
3A	19.5	2754	6173	71.02	288	358	320	807	5885	5815	5853	5366	#1) 1.097 #2) 1.114 #3) 1.107 #4) .413	1.106
3B	19.7	2658	6072	68.58	227	234	203	863	5845	5838	5869	5209	#1) 1.067 #2) 1.070 #3) 1.068 #4) .408	1.068

TABLE 9, Con't., Page 2

Remarks:

1) *Indicates data obtained from NACA TN 4265, Composition and Thermodynamic Properties of Air in Chemical Equilibrium, W. E. Moeckel & Kenneth C. Weston, Lewis Flight Propulsion Laboratory, Cleveland, Ohio, April, 1958.

2) Calculated in same way as shown in Table 5.

3) Thermocouple #4 burned through - not included in average Keff.

APG Test Specimen Sketch

(4" x 1" x .500")

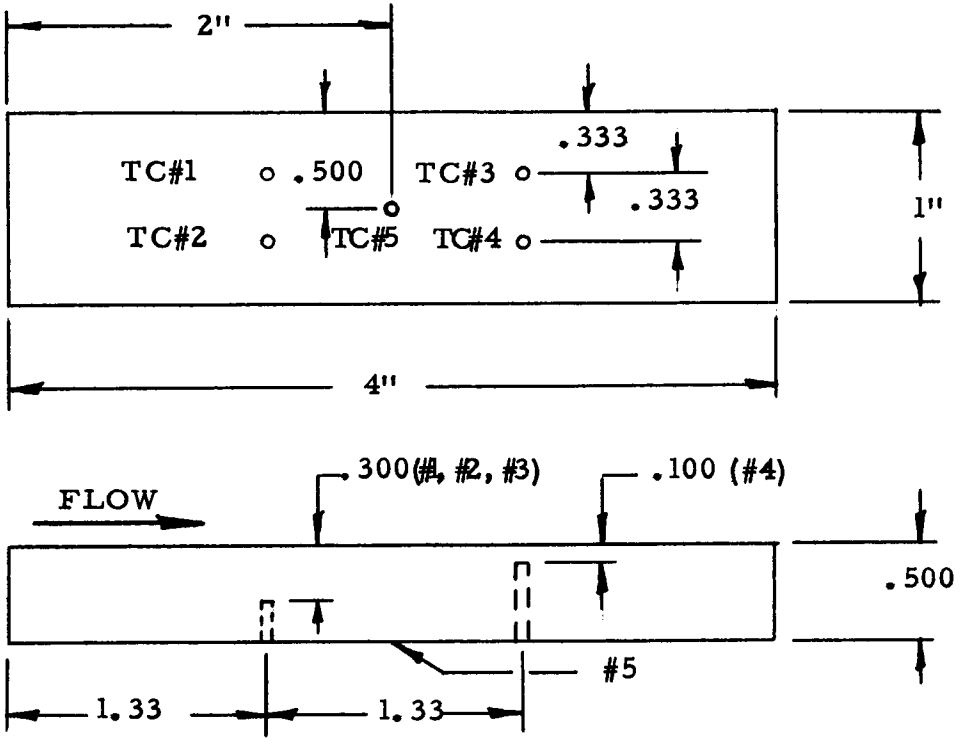

Simultaneously with the fabrication and testing of these composite materials, CTL was developing and proof testing an "Analytical Procedure for the Weight Percentage Determination of the Fibrous and Resinous Constituents of Composite Test Panels" as described in Appendix 3. This procedure was applicable to both the finished mats and finished molded composite test panels. Check tests were conducted on the finished mats to determine if the theoretical pre-selected fiber compositions were achieved. Analyses were also performed on the finished composite test panels in order to accurately determine if the theoretical pre-selected composites were achieved and to plot the exact data location for each composite. The actual fiber and resin constituent percentages obtained by using this analytical method are listed in Table 6.

Using this data parametric charts were prepared, as evidenced by test panel data locations 1A through 3B on Figure Nos. 11 through 18. These charts on the longer fiber composites indicated some improvement in the surface contour or geometric configuration over the previous charts for the thermal conductivity, specific heat, and mass loss rate properties. This improvement was attributed to the better distribution of fibers and reduced fiber losses during mat processing. Yet, it was very evident that the same basic control problems, considered in the Discussion of Results section of this report, were still in existence in the processing and testing of these repeat test panels.

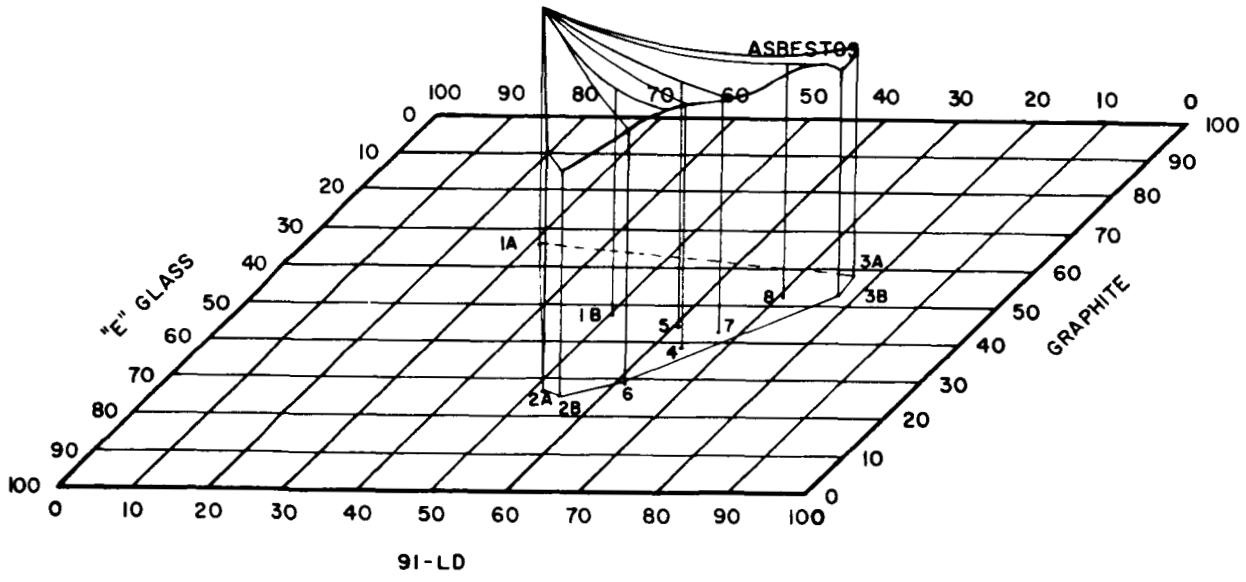

FIGURE NO. 11 PARAMETRIC CHART FOR DENSITY

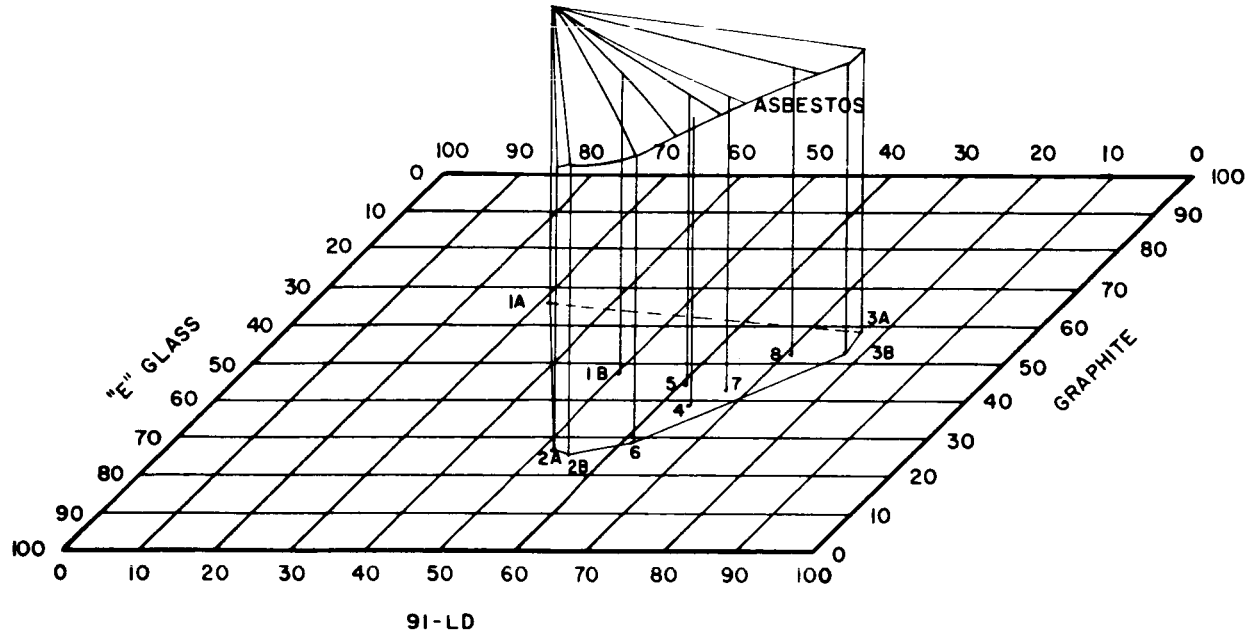

FIGURE NO. 12 PARAMETRIC CHART FOR SPECIFIC HEAT

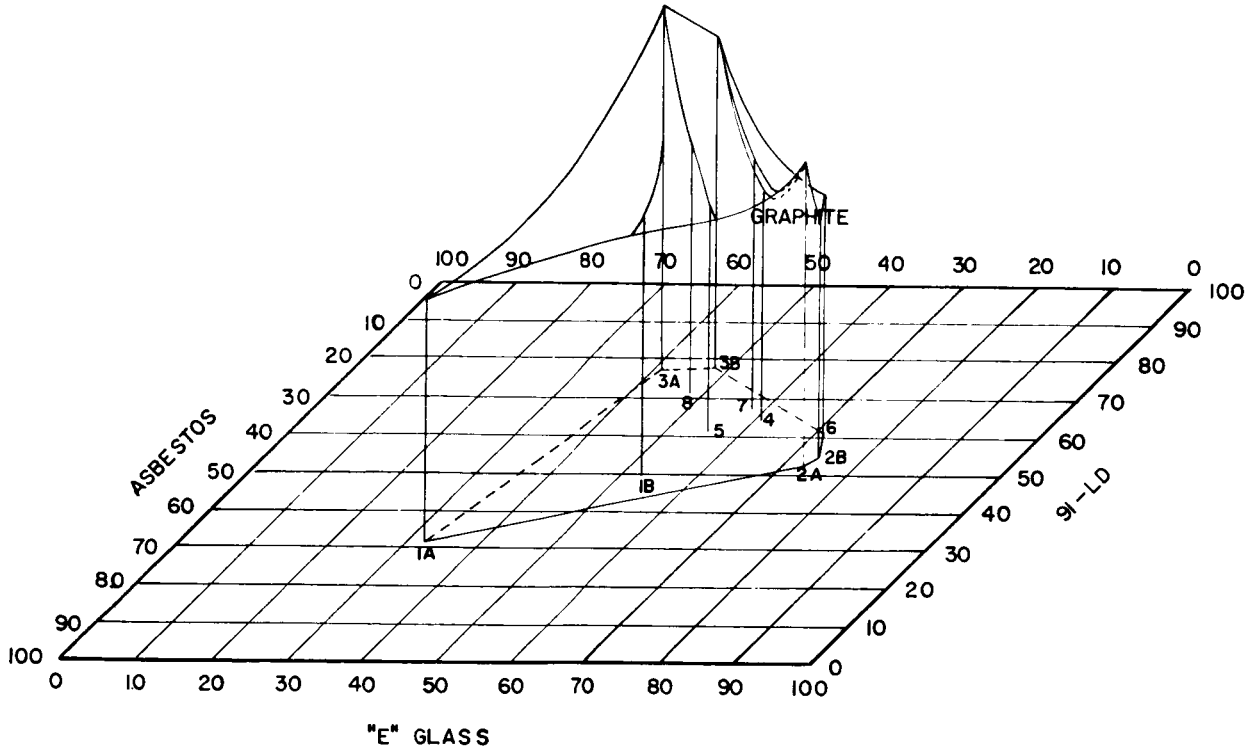

FIGURE NO. 13 PARAMETRIC CHART FOR THERMAL CONDUCTIVITY

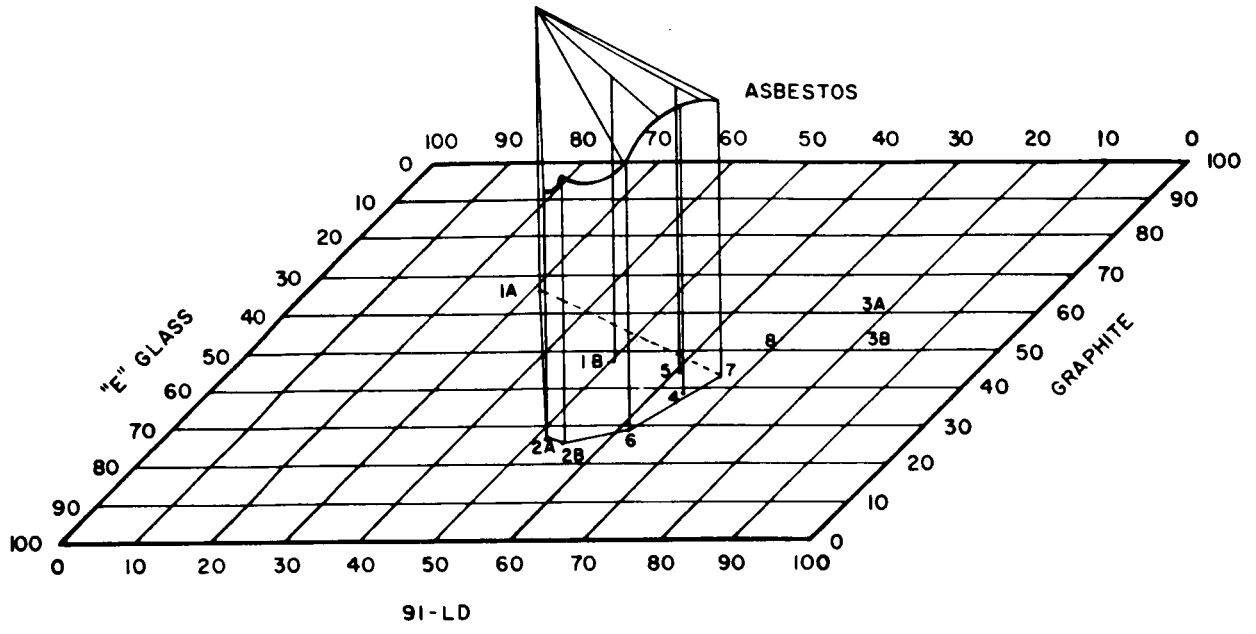

FIGURE NO. 14 PARAMETRIC CHART FOR MELTING POINT

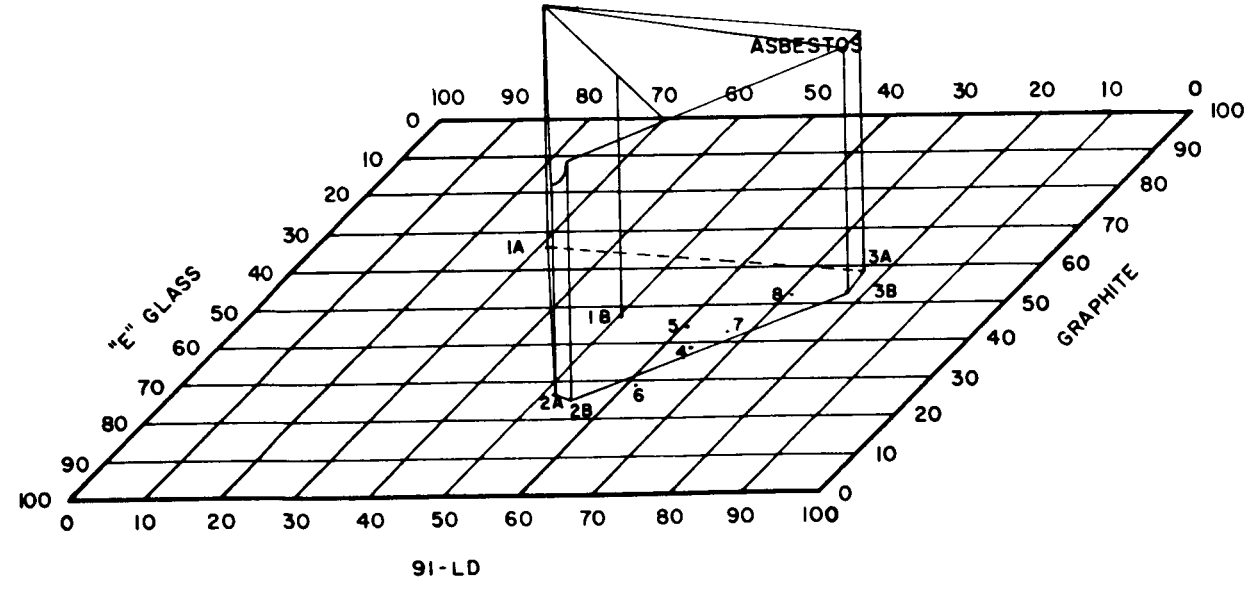

FIGURE NO. 15 PARAMETRIC CHART FOR EMISSIVITY

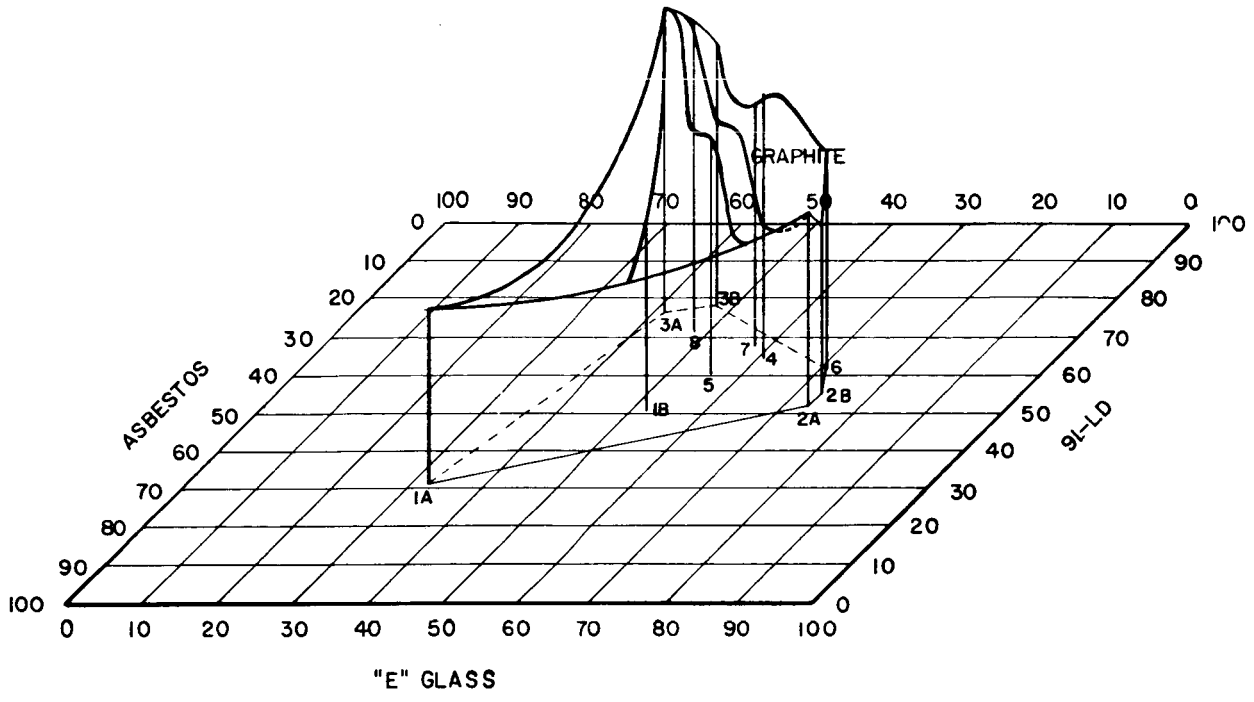

FIGURE NO. 16
PARAMETRIC CHART FOR EFFECTIVE HEAT OF ABLATION

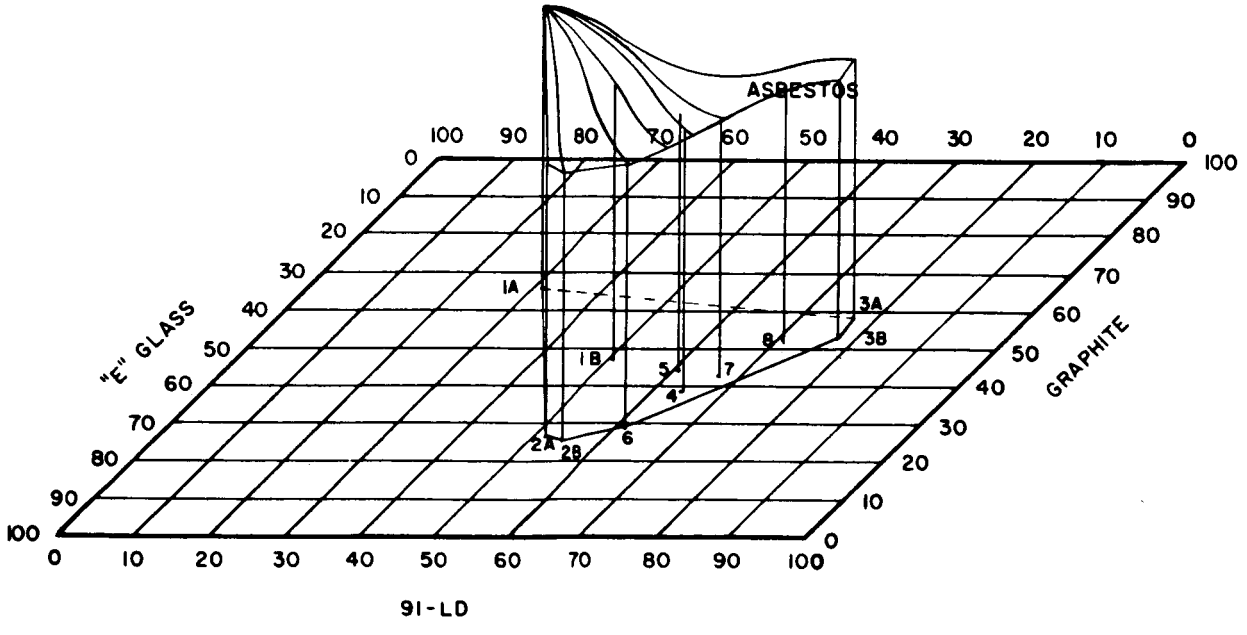

FIGURE NO. 17 PARAMETRIC CHART FOR MASS LOSS RATE

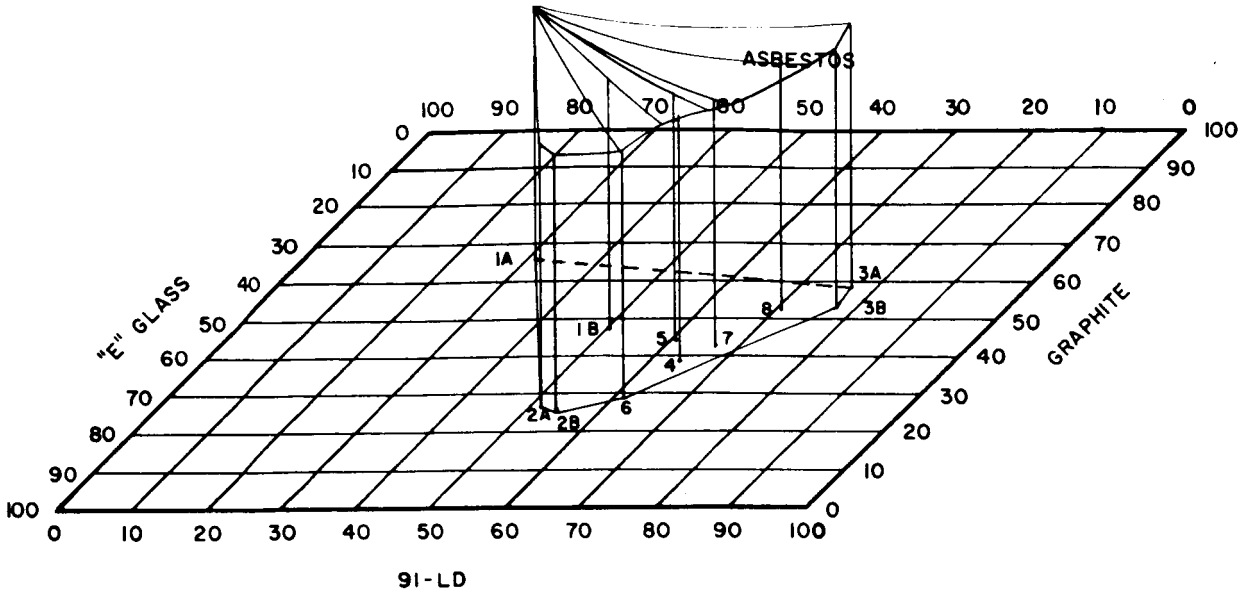

FIGURE NO. 18

PARAMETRIC CHART FOR EFFECTIVE THERMAL CONDUCTIVITY

In order to correct these faults CTL searched for other processing equipment which would be better suited for the production of future experimental mats. Such equipment was located and is described fully in Appendix 1 under the title Rando-Feeder and Rando-Webber Fibrous Web System.

In order to further define the geometric configuration of the partially developed parametric charts, five randomly located points on the charts were selected. These points denoted specific materials compositions that when plotted would lie within the analytically determined composite data locations previously established and designated as 1A through 3B. These five composites were to be formulated to the following theoretical pre-selected materials (by weight) compositions:

Composite No.	% Resin	% Asbestos	% Glass	% Graphite
4	47.5	17.5	17.5	17.5
5	40.0	40.0	5.0	15.0
6	35.0	10.0	40.0	15.0
7	45.0	25.0	5.0	25.0
8	45.0	10.0	5.0	40.0

To prepare composites having the above materials compositions, it was calculated that mats would have to be prepared according to the following theoretical fiber weight schedule:

Mat No.	% Asbestos	% Glass	% Graphite
4	33.33	33.33	33.33
5	66.66	8.33	25.00
6	15.40	61.50	23.10
7	45.45	9.10	45.45
8	18.20	9.10	72.70

These mats were processed on the Rando-Feeder and Webber equipment as described in Appendix 1. Fifteen pound batch formulations were produced as 20 yard length by 40 inch width mats that were controlled to a uniform weight of 9 ounces per square yard. These mats exhibited excellent uniformity, fiber dispersion, and were readily handled without the aid of a binder system. This was in marked contrast to the mats previously made on the Proctor equipment. Mats 5 and 1 are typical of the ones produced by these two different processes and are presented in Figure Nos. 19 and 20 for comparison purposes.

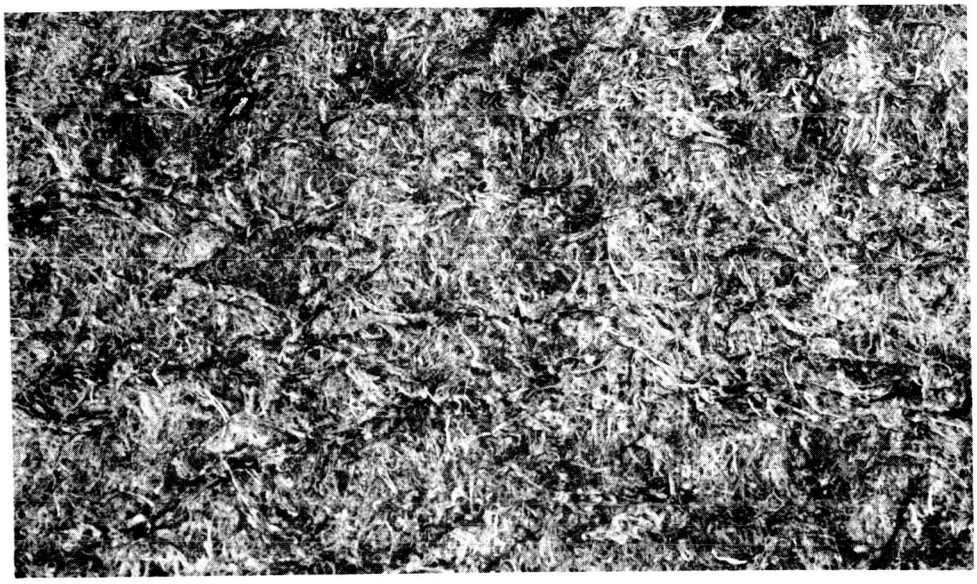

FIGURE NO. 19
MAT NO. 5 PROCESSED ON RANDO EQUIPMENT

FIGURE NO. 20
MAT NO. 1 PROCESSED ON PROCTOR EQUIPMENT

The same resin impregnation method used on the previous mats was applied to these mats. Test panels that were to be of the formulations listed for the aforementioned composite numbers , 4 through 8, were fabricated. Test specimens were prepared and testing was conducted in the same manner as before. Typical APG test specimens are shown in Figure No. 21 in the before and after firing conditions.

FIGURE NO. 21 TYPICAL APG TEST SPECIMENS

The analytical procedure described in Appendix 3 was applied to these composites and the results are tabulated in Table 10. This table lists weight constituent percentages and summarizes all properties data for all the long fiber composite materials processed during this program. Tables 11, 12 and 13 present the supporting data and descriptive information on composites 4 through 8.

TABLE 10

LONG FIBER COMPOSITES AND THEIR PROPERTIES

A. Constituent Percentages by Actual Analyses

Composite No.	% 91LD Resin	% Asbestos	% "E" Glass	% Graphite
1A	26.53	67.00	5.20	1.27
1B	47.93	47.05	4.00	1.02
2A	38.04	10.81	47.85	3.30
2B	43.07	8.89	44.78	3.26
3A	46.81	3.06	2.69	47.44
3B	54.44	2.11	2.17	41.28
4	52.59	15.32	20.50	11.59
5	53.88	30.88	5.83	9.41
6	45.79	4.15	40.10	9.96
7	57.37	19.50	5.86	17.27
8	48.93	9.26	6.74	35.07

B. Composite Properties

Composite No.	Density (lbs/ft^3)	Specific Heat @ 500°F (BTU/lb.°F)	Thermal Conductivity @ 500 °F (BTU/hr/ft°F	Melting Point (°F.)	APG TESTS			
					Emissivity	Effective Heat of Ablation (BTU/lb.)	Mass Loss Rate (lbs/ft^2sec)	Effective Thermal Conductivity (BTU/ft.hr.°F)
1A	89.4	.344	.182	2260	.936	3,691	.0188	1.016
1B	78.6	.358	.214	2255	.923	4,016	.0181	1.006
2A	90.7	.258	.288	1945	.686	5,342	.0141	1.122
2B	78.7	.305	.170	2140	.907	3.431	.0177	1.050
3A	83.5	.272	.382	-	.917	14,428	.0049	1.106
3B	80.4	.319	.326	-	.961	11,531	.0055	1.068
4	96.3	.297	.152	2260	-	11.935	.0061	.950
5	95.9	.319	.156	2265	-	8,767	.0070	.950
6	101.1	.285	.176	2080	-	7,999	.0075	.956
7	87.5	.331	.194	2190	-	9,325	.0065	.945
8	86.5	.293	.194	-	-	14,175	.0045	.972

TABLE 11

EFFECTIVE HEAT OF ABLATION TEST DATA

Composite No.	Cold Wall Heat Rate $\left(\frac{BTU}{ft^2 sec.}\right)$	Power Input $\left(\frac{BTU}{sec.}\right)$	H_2O Mass Flow $\left(\frac{lbs}{sec.}\right)$	H_2O Temp Increase (^oF)	Hot Wall Temp. (^oF)	Hot Wall Enthalpy $\left(\frac{BTU}{lb.}\right)$	Mass Flow $\left(\frac{lbs}{sec}\right)$	Recession Rate $\left(\frac{ft}{sec}\right)$	Density (lbs/ft^3)	Eff. Heat of Ablation (BTU/lb)
4	89.4	307	27.98	9.86	2430	758.55	.01229	.000064	96.3	11,935
5	89.4	307	27.63	10	2475	771.68	.01268	.000073	95.9	8,767
6	89.4	307	27.9	10	2395	748.33	.01227	.000074	101.1	7,999
7	89.4	306	27.63	10	2480	774.60	.01241	.000075	87.5	9,325
8	89.4	306	27.63	9.95	2410	743.96	.01223	.000052	86.5	14,175

Remarks:

1) Test gas was 80% Nitrogen with 20% Oxygen injected downstream of the arc.

2) Hot wall gas enthalpy values were obtained from Table 7, Thermodynamic Properties of Dry Air, Aircraft and Missile Propulsion, Volume I, M. J. Zucrow, John Wiley & Sons, Inc., 1958.

3) Actual time that mass loss was experienced, as determined from movie films of the test runs, was employed.

4) Calculated in same way as shown in Table 3.

TABLE 12

MASS LOSS RATE TEST DATA

Composite No.	Density (lbs/ft^3)	Exposure Duration (seconds)	Spec. Wt. Before Firing (grams)	Total Mass Loss (grams)	Total Mass Loss (%)	Total Ablation (inches)	Recession Rate (in./sec.)	Mass Loss Rate ($lbs./ft^2$ sec.)
4	96.3	78.5	52.8267	7.5068	14.2	.0596	.00076	.00612
5	95.9	73.4	51.4490	7.6914	15.0	.0640	.00087	.00696
6	101.1	76.8	54.5509	7.1620	13.1	.0680	.00089	.00747
7	87.5	73.5	48.2822	7.8562	16.3	.0660	.00090	.00654
8	86.5	90.0	46.0103	9.3973	20.5	.0560	.00063	.00448

Remarks:

1) Actual time that mass loss was experienced, as determined from movie films of the test runs, was employed.

2) Calculated in same way as shown in Table 4.

TABLE 13

EFFECTIVE THERMAL CONDUCTIVITY TEST DATA

Composite No.	Chamber Pressure (psi)	Gas Enthalpy (BTU/lb.)	Gas* Temp (°F)	Hot Wall Heat Rate (BTU/ft² sec.)	Temp. °F @ TC Location after 30 seconds				Gas Temp. minus TC Temp. in °F				Keff@TC Location (BTU/ft hr °F)	Keff Average (BTU/ft hr °F)
					TC#1 (.3" Deep)	TC#2 (.3" Deep)	TC#3 (.3" Deep)	TC#4 (.1" Deep)	TC#1 (.3" Deep)	TC#2 (.3" Deep)	TC#3 (.3" Deep)	TC#4 (.1" Deep)		
4	19.7	2593	6000	62.9	90	90	90	202	5910	5910	5910	5798	#1) .950 #2) .951 #3) .950 #4) .337	.950
5	19.7	2425	5815	60.97	86	85	86	200	5729	5730	5729	5615	#1) .956 #2) .952 #3) .942 #4) .332	.950
6	19.3	2240	5602	59.47	86	85	88	213	5516	5517	5514	5389	#1) .957 #2) .953 #3) .959 #4) .330	.956
7	19.3	2438	5823	60.99	93	92	93	215	5730	5731	5730	5608	#1) .943 #2) .942 #3) .949 #4) .329	.945
8	19.2	2535	5926	63.15	121	108	139	222	5805	5818	5787	5704	#1) .973 #2) .962 #3) .982 #4) .330	.972

Remarks:

1) *Indicates data obtained from NACA TN 4265, Composition and Thermodynamics Properties of Air in Chemical Equilibrium, W. E. Moeckel & Kenneth C. Weston, Lewis Flight Propulsion Laboratory, Cleveland, Ohio, April, 1958.
2) Calculated in same way as shown in Table 5.
3) Thermocouple #4 not included in average Keff.

APG Test Specimen Sketch - same as is shown in Table 9.

Using these test results, the geometrical configuration of the planes of the parametric charts were defined. By placing the same components in the same side locations on each property chart, the five randomly located points were maintained at the same base or plan view locations throughout the series of charts. Naturally all of the desired materials compositions for these composites could not be achieved due to fiber losses during processing. Also due to budget limitations not enough material was available to develop absolute, controlled procedures for the impregnation and B-staging operations. Figure No. 22 demonstrates the desired or theoretical data point locations on the parametric chart base or plan view. The actual data point locations for these composites as determined by the Appendix 3 analytical procedure, are included on this figure for comparison versus the theoretically desired materials compositions. This comparison clearly shows that such an analytical procedure is absolutely necessary for proper data point location and surface contour definition of the parametric charts.

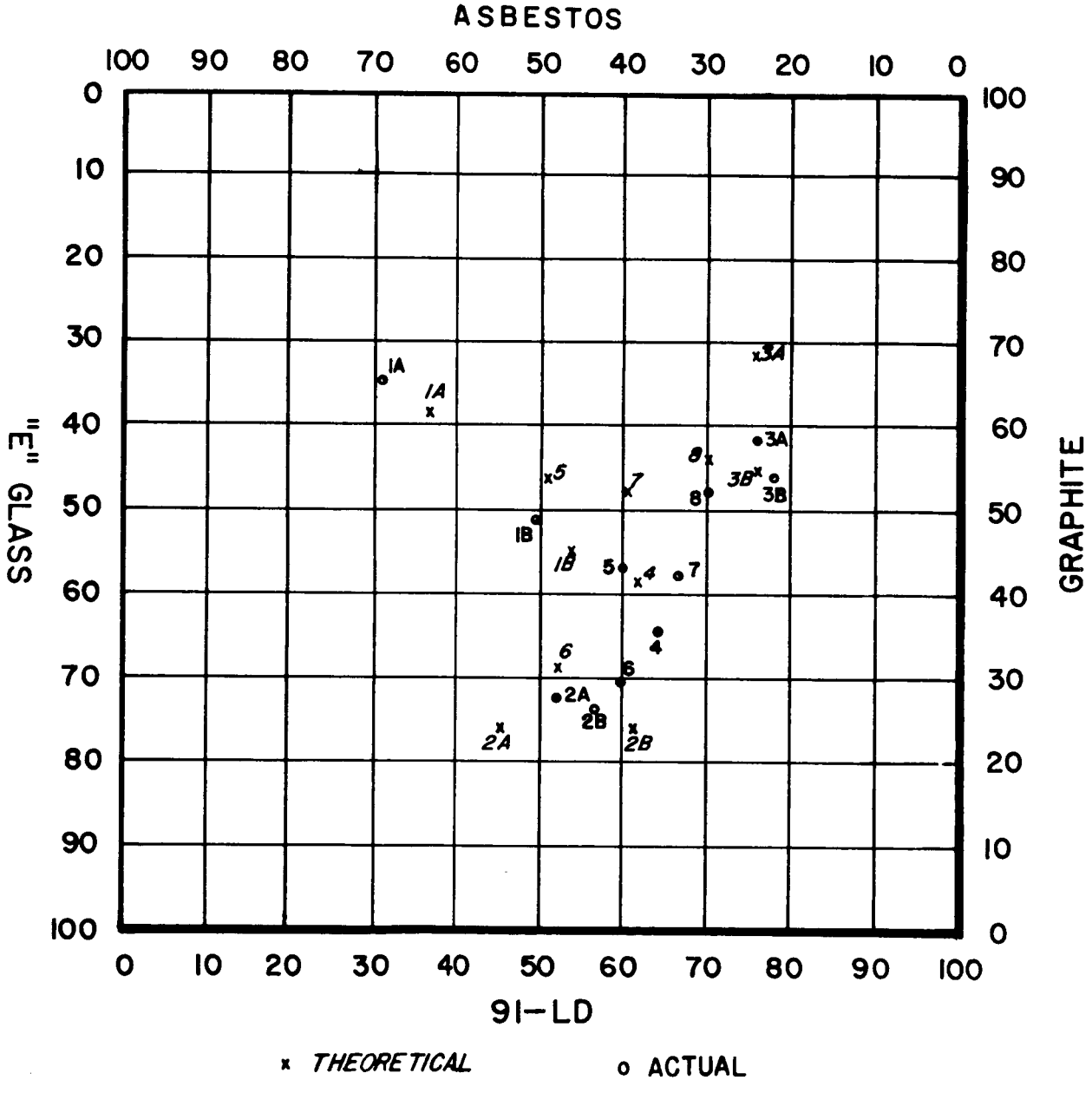

FIGURE NO. 22 PRE-SELECTED COMPOSITE LOCATIONS VS. ACTUAL LOCATIONS

The results of these analyses and the data obtained from the various properties determinations were used to parametrically chart and define the surface contours of the planes of the parametric charts. These charts, Figure Nos. 11 through 18, established the validity of the charting portion of the MPT.

PARAMETRIC CHART CONSTRUCTION AND DEVELOPMENT

The purpose of the parametric charts is to provide a graphical method which will indicate the relationship between any particular weight combination of the four constituents in the system and the particular property data or value being investigated for that particular weight combination.

The individual charts are constructed by employing a parallelogram as the chart base as previously shown in Figures 11 through 18. Each side of the parallelogram represents one of the constituents of the system and is scaled to indicate 0 to 100% by weight of that constituent. The weight percentage of each constituent is located on its respective side scale and lines are drawn to connect the opposite sides at these locations. The point of inter-section of these lines on the chart base becomes the location at which the property data determined for the particular weight combination of constituents is placed. The property data point location for each composite material investigated is plotted in this manner.

Property values obtained by experimental determinations on these composite materials are then represented on the chart by constructing scaled, vertical lines at these data point locations. When all of the values for all of the properties on the materials composites under study have been determined and represented in this manner, a topographical map of the region bounded on the chart is generated by connecting these vertical scaled data lines. The resultant three dimensional, geometric configuration can then be used to predict property values for other theoretical or selected weight combinations of these constituents or materials composites that would lie within the charted region.

These developed charts are employed in CTL's Material Prediction Technique (MPT), in the following way, to predict properties of composite materials that will function properly in the hypothetical thermal environment being considered. The major portion of the MPT program is applied to a computer in a manner which samples the effect of varying materials properties against the performance parameters (of the body or part under design consideration) so as to derive the idealized materials properties necessary for proper behavior of the part.

Computer analysis entailing iteration processing is used for rough cut determinations of the idealized, yet practical, property values that are required to satisfy the hypothetical thermal environment. These data or values are established on the bases of the charts at the location(s) where their vertical, scaled property lines mate with the pre-established (by the empirical data determinations) surface contour of the chart. Intersecting

lines are then drawn across the established location(s) to determine a number of possible various, practical weight combinations of constituents for composite materials that will satisfy the computer determined, idealized property value.

After these procedures are completed for all of the charts and properties being examined, a cross correlation of all of the individual charts is made to develop a composite material. In this process each of the various parameters is optimized by varying the weight combinations of the constituents and the processing history in accordance with the mode and composition predicted by the cross correlation. By rotation of the intersecting lines and points, a compromise composite material which incorporates most of the properties into one composite blend or mix is achieved. In other words, a center of gravity, axis of rotation solution for determination of this optimum blend point or region is employed. This consolidation technique is demonstrated by Figure No. 23. This optimized composite is then processed and exposed to the selected hypothetical thermal environment to compare predicted performance with actual materials performance.

POSSIBLE BLENDS OF MATERIALS

	1	2	3	4	5	6	7	8	9	10	11	12	13	14
91-LD	100	100	100	90	85	90	80	70	60	60	60	60	60	80
"E" GLASS	80	40	10	80	80	30	70	80	80	80	60	50	50	60
ASBESTOS	20	10	60	10	20	60	40	20	50	30	40	60	30	30
GRAPHITE	20	50	30	20	15	10	10	30	10	30	40	30	60	30

NUMBER 14 IS EXPERIMENTAL BLEND

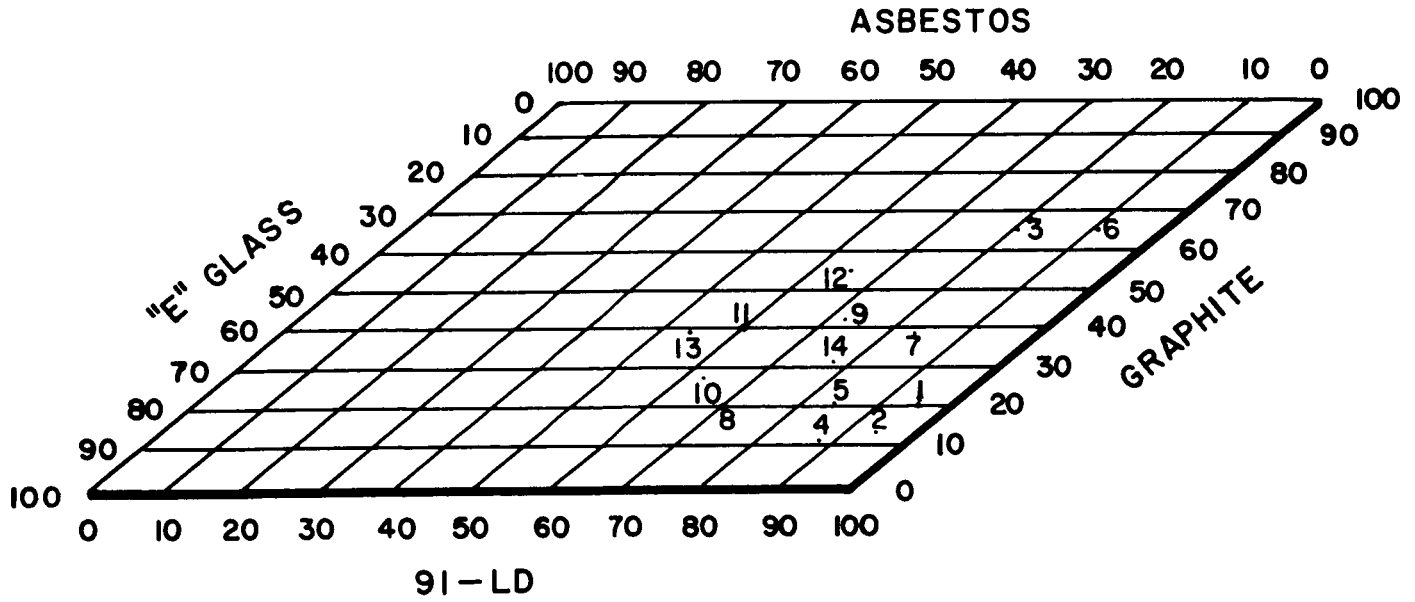

FIGURE NO. 23 PARAMETRIC CHART CONSOLIDATION TECHNIQUE

There are some practical problems encountered in establishing the properties data required for the development of these parametric charts. Some of these properties can be established with little or no difficulty. For example, consider the property of density. Density values which are determined under a specified environment on the constituents in their virgin or raw material form will provide very good, accurate data. When this type of data is used in constructing the parametric chart for this property, it provides an evenly defined, uniform surface contour. This type of topographical chart development yields quick, accurate prediction of density values for any selected weight combination of constituents in a composite material. It is evident that this particular property is one which is, practically speaking, independent of environmental factors and as such will function well in this technique.

To the contrary, a property such as thermal conductivity is strongly dependent on many physical and environmental factors, such as fiber size, fiber orientation, porosity, density, processing procedures, etc. It becomes absolutely necessary then to conduct data determinations on the reinforcements in conjunction with binder or resin matrix material. Normally, separate specimens are prepared, in addition to the mats, from each fibrous reinforcement selected and from the binder material. The singular fibrous reinforcement specimens consist simply of the loose fibers and are only processed into mat form if it is necessary for facilitation and proper interpretation of properties testing. All specimens are fully cured, including the binder specimen, prior to data determinations.

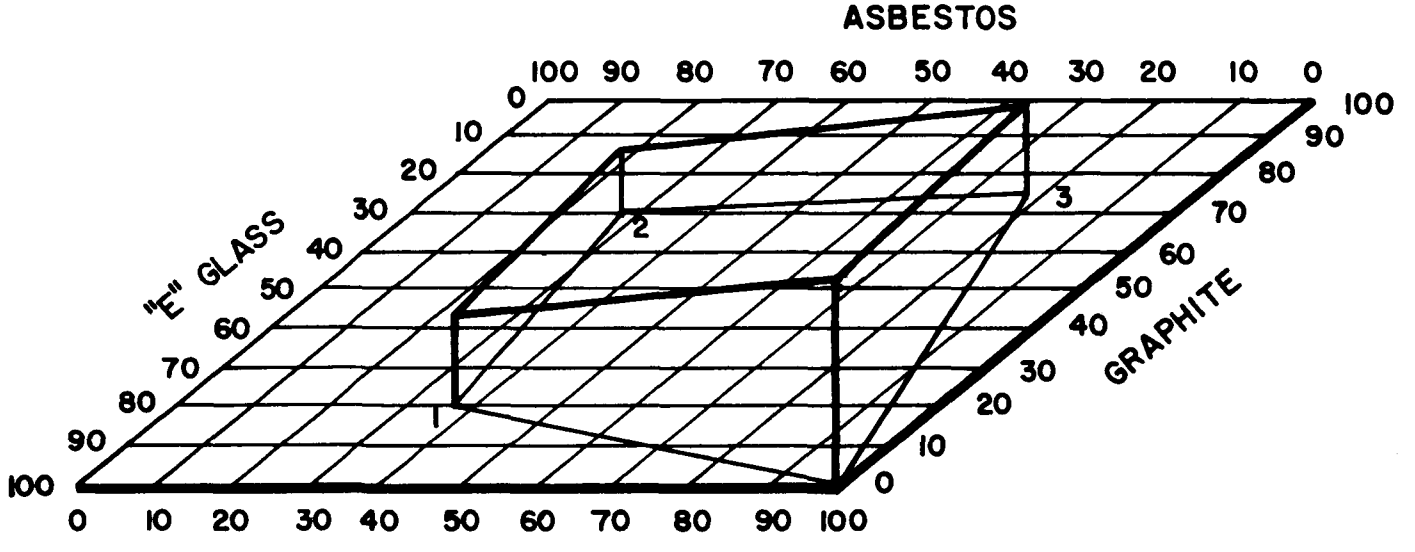

	1	2	3
91-LD	20	20	20
ASBESTOS	70	5	5
"E" GLASS	5	70	5
GRAPHITE	5	5	70

FIGURE NO. 24 RESIN-REINFORCEMENT DILUTIONS RELATED TO VIRGIN CORNERS

By adhering to the above procedures the influence on the test data of both the physical and chemical inter-relationship of the constituents of the composite is taken into account, thus yielding realistic data. In some cases, it is possible to broaden the useful area, perhaps even the complete area, of the chart. This can be done by relating the surface configuration to the one constituent which can be determined in its pure form. Such a technique is exemplified in Figure 24.

The above paragraphs indicated the manner in which the fully developed parametric charts are employed with the Material Prediction Technique. Under this contract the only objective was to demonstrate the validity of the parametric charting portion of this technique.

In this program all of the data accumulated in this way on the preselected composites 1A through 3B, was used as the initial step in the surfacearea definition of the parametric charts. The data on the five randomly located, selected composites, 4 through 8, was then used to further define this area and the geometrical configuration of the planes of these parametric charts. These selections of composite combinations were made with practical materials and manufacturing limits (maximum and minimum levels) used as the criteria for establishment of the useable area of the charts. In accordance with the procedures in the preceding paragraphs, these properties data were established as scaled vertical lines, with the bases of the lines at the proper data point locations on the base of the charts and the tops of the lines defining the warp plane of the charts.

The test results for the eight individual types of property determinations are listed in Table 10. These results were used to provide the graphical charting method, demonstrated in Figure Nos. 11 through 18, which ultimately indicates the relationship between any particular weight combination of the constituents of the composite system and the property value for that particular combination. It was decided by NASA-GCMSFC personnel that this charting technique-optimization procedure would be applied to an actual radiant/convective thermal insulation problem and work with the materials being used in this program would be discontinued. This will be done instead of continuing the program on the hypothetical convective environment basis.

DISCUSSION OF RESULTS

The value of the parametric charts and the Material Prediction Technique is dependent upon the consistency and accuracy of the processing and testing procedures which are employed. For these reasons, it is absolutely necessary to be able to affect proper processing controls during the blending or non-woven mat manufacture and during the impregnation and test panel fabrication operations so as to produce uniform test materials and accurate test results.

These facts were very evident with the manufacture of the initial experimental mats using the Proctor textile processing machinery. Excessive fiber losses were experienced on this equipment whether short or long fibrous reinforcements were used. The use of long fibers resulted in some improvement in this respect since better transfer through the garnett and better secondary fiber dispersion was noted. This non-uniformity, however, was due to the very nature of the fibers, the textile equipment being used, and the fact that very small batch (7 to 21 lbs. vs. hundreds for production batches) blends were necessarily, due to monetary limitations, investigated.

It was very likely, in these small batch matting operations, that the small amounts of incompletely opened secondary fibers that were not lost during the picking, condensing, conveying and garnetting operations and remained in the blend were deposited non-uniformly in the mat veils. These problems were especially manifested in the blends that employed the graphite fibers as the major constituent since the secondary asbestos and glass fibers were not carried very well by the graphite fibers.

These processing problems just described produced localized excesses and absences of the secondary fibers in the resultant mats. Consequently, physical properties data irregularities definitely do occur when the small, individual test specimens are cut from these areas of the test panels and this data can vary widely within these panels. Material compositions 1A through 3B, in Figure Nos. 11 through 18, and their experimentally determined property values display these data inconsistencies due to localized constituent abnormalities.

The five randomly located material compositions, 4 through 8, in Figure Nos. 11 through 18, were used for further definition of these parametric charts. The data obtained for these composites was much more consistent and reliable and provided regular chart contours. The use of the Rando textile equipment in the production of these mats practically eliminated fiber losses and insured complete, uniform dispersion of the secondary fibers under closely controlled manufacturing procedures.

As was stated previously, the optimization of each individual property chart and the cross correlation of these charts must be performed with the processing histories of the individual composite materials being taken into account. For example, Table 14 lists the theoretical or calculated density values (based on actual air comparison pycnometer data determined on the virgin constituents) versus the actual or experimentally determined density values for the composite materials 1A through 9. Actual densities were obtained by two different methods. That is, by the air comparison pycnometer method and by the standard ASTM dry weight/measurement method. A correlation of the actual values versus the theoretical density values was made. This was expressed as the percentage of the maximum or theoretical density possible which was achieved in the composite material test panel.

TABLE 14

% OF THEORETICAL DENSITY ACHIEVED IN COMPOSITES

A. Pycnometer Measurements of Density of Constituents

1) 91LD Phenolic Resin (cast) 71.7 lbs/ft^3
2) Asbestos (Chrysotile) fibers 146.8 lbs/ft^3
3) "E" Glass fibers 154.5 lbs/ft^3
4) Graphite (WFA) fibers 97.6 lbs/ft^3

B. Actual vs. Theoretical Density of Composites

Composite No.	Actual (By ASTM)	Theoretical (Based on Pycnometer Data)	Actual (By Pycnometer)	% of Theoretical (By Pycnometer)
1A	89.4 lbs/ft^3	127.14 lbs/ft^3	118.0 lbs/ft^3	92.8
1B	78.6 " "	110.52 " "	110.0 " "	99.6
2A	90.7 " "	120.32 " "	118.8 " "	98.1
2B	78.7 " "	116.63 " "	97.0 " "	83.4
3A	83.5 " "	88.56 " "	88.4 " "	99.7
3B	80.4 " "	86.46 " "	86.2 " "	99.8
4	96.3 " "	103.20 " "	99.3 " "	96.1
5	95.9 " "	101.98 " "	98.0 " "	96.2
6	101.1 " "	112.20 " "	112.1 " "	99.9
7	88.8 " "	95.58 " "	93.2 " "	97.4
8	86.5 " "	93.30 " "	92.7 " "	99.4

The theoretical density values were calculated on the basis that the value of a property of a composite material is an additive function of that property in the constituent materials. This is assumed to be the case for properties where intimate blending of the constituent materials is achieved without interactions between materials. The general equation for such a property in composite materials is:

$X = W_1 x_2 + W_2 x_2 + W_3 x_3 + W_4 x_4$, where

X is the value of that property in the composite material,
x is the value of the property for the constituent designated by the subscript number, and
W is the weight fraction of the constituents designated by the subscript number. The sum of the W values in the equation must equal unity.

Examining the individual property charts, in the light of the actual densities achieved with the composite material test panels and other processing factors involved, elicits the following comments on the geometric configuration of the parametric charts.

The chart for the property of density discloses a very uniform, regular surface contour. The only data value which deviates greatly from this contour is that for composite 2B and the value or percent of theoretical density achieved for this composite is the most widely discrepant of all the composites plotted.

The chart for the property of specific heat exhibits a very uniform, slightly irregular surface contour. Again, the only data value which departs from this uniformity is that for composite 2B. This value departure also serves as an explanation for the contour irregularity at that point.

The chart for the property of thermal conductivity appears as a non-uniform, somewhat irregular surface contour. It was explained, earlier that this property is very easily influenced by changes in density, porosity (due to processing methods) and fiber orientation. Considering these factors, it is reasonable to assume that the irregularity of the warped surface plane was due to the inability to produce test panels that closely approximated the theoretical densities calculated for composite test panels 2B, 1A, 4 and 5. These lower density panels indicate lower thermal conductivity data values which correspondingly result in the irregularities noted at these locations on the chart.

The charts for the properties of melting point and emissivity are incomplete. Data could not be obtained on all the composite test specimens since the values were beyond the established ranges of the recording pyrometers and instrumentation. However, the areas defined on these charts by the determined data materialize as very regular, uniform surface contours.

The chart for the property of effective heat of ablation unveils some-

what the same type non-uniform, irregular surface contour as evolved with the thermal conductivity chart. Here, too, the deviations in densities for composites 2B, 1A, 4 and 5 from the calculated densities caused the irregularities in the surface contour of this chart. Fiber orientation differences between the 1A through 3B specimens and the 4 through 8 specimens also added to the surface contour variations. Generally, the fibers in the 1A through 3B specimens oriented themselves parallel to the surface while in the 4 through 8 specimens the fibers were more perpendicular to the surface. Use of fabrics rather than non-woven mats would eliminate this difficulty.

The chart for the property of mass loss rate sets forth a fairly regular, uniform surface contour. The slight irregularities produced by the 1A through 3B composites are probably caused by the differences in fiber orientation that resulted in higher mass loss rates.

The chart for the property of effective thermal conductivity produced an almost perfectly uniform, regular surface contour.

COMMENTS AND RECOMMENDATIONS

In general, the parametric charts which were developed for the materials being investigated in this program demonstrated the practicality and validity of such a technique for use in predicting properties of materials in selected composite forms. The developed charts exposed definite properties trends that would aid in the selection of materials for a particular application. Many of the anticipated problem areas were uncovered, resolved, and have established guidelines for future work with binders and reinforcements.

It was apparent during this program that production processes and equipment can be employed with these techniques. But, it is absolutely necessary that proper and effective blending of the constituent materials be accomplished under pre-established control procedures. This is imperative for accurate location of the data points for the composites under study and ultimately for the correct definition of the geometric configuration of the parametric charts. The procedures used for preparation of the test panels and test specimens must be conducted according to a pre-determined standardized method which is properly equated to some guiding criteria such as theoretical density.

It is felt that future investigation of thermal conductivity, mass loss rate, and effective heat of ablation, etc., should be carried out on test specimens made with fabrics woven from yarns spun from the blended fibers. Use of fabrics would provide very close control during impregnation with the binder and allow perfect orientation of the materials. It would also yield accurate processing controls during fabrication. The combined improvements from these changes would yield uniform, regular parametric chart surface contours.

All future testing should be conducted on a minimum of five individual tests per material per property being determined. This will provide better data reliability than was originally obtained. Test methods and conditions should be pre-set and maintained throughout the program.

All of the above recommendations, if adhered to, will insure that uniform and accurate parametric chart surface contour definition is produced since good correlation and complete corroboration of data can be obtained.

Based on the above discussions, it is recommended that this technique be applied to an actual thermal insulation problem such as might be encountered on the SATURN vehicle.

It is also recommended that the parametric approach to material properties, as used with the Material Prediction Technique, be put on a "computerized" basis. The geometrical "warped" surfaces used at present to represent the physical properties of material composites would be replaced by sets of mathematical equations that could include the variations of the properties with temperatures.

APPENDIX 1

PROCEDURES FOR MANUFACTURING NON-WOVEN FIBROUS MATS

The three basic fibers employed in this program were blended and processed into a usable raw material form as non-woven mats by using the two different types of textile equipment and processing described below.

These processes are capable of providing material in forms other than the continuous mat form described in this program. The material can be made as a thick non-continuous batt and also as a roving which can subsequently be twisted and spun into yarn for weaving into conventional fabrics on standard textile looms.

PROCTOR AUTOMATIC MAT MAKING SYSTEM

The equipment used here consisted of basic textile processing machinery made by Proctor and Schwartz, Inc., Philadelphia, Pennsylvania. The actual blending of the raw fibers into mat forms was accomplished in the following manner at the existing facilities of the North American Asbestos Corporation at Mundelein, Illinois.

The various fibers were properly weighed in individual hoppers (Figure 25) and conveyed to a picker and condenser (Figure 26) and then taken overhead by the conveyor to the hopper of a garnett. This process was supposed to break apart any fiber bundles that existed and blend these separated fibers to achieve a uniform mixture. The garnett (Figures 27 and 28) weighed, combed, and laid a thin veil of fibers on a slat conveyor. This conveyor carried the veil up and over the camel back (Figure 29) where a crosser laid the veil in a uniform pile, consisting of a number of layers, onto a moving conveyor belt, or Fourdrinier screen, where it was wetted with a mixture of solvent and phenolic resin (Figure 30) which subsequently acted as a preliminary binder. The excess solution was pulled off with a vacuum and the wetlap (Figure 31) was transferred by the conveyor belt into a traveling oven for curing (Figure 32). The oven dried and fixed the small amount of resin to a "C" stage condition so that the mat could be handled for future processing. As it emerged from the oven it was put up in rolls (Figure 33).

This process is a proven production (as several hundred pound batches) procedure with only manufacturing adjustments normally being made depending upon the composite material to be manufactured. Usually this is comprised of achieving the proper feeds and speeds of the conveyor system. However, with the small amount or weights of the fibers being employed in this program further adjustments and equipment modifications would have been necessary to produce high quality mats.

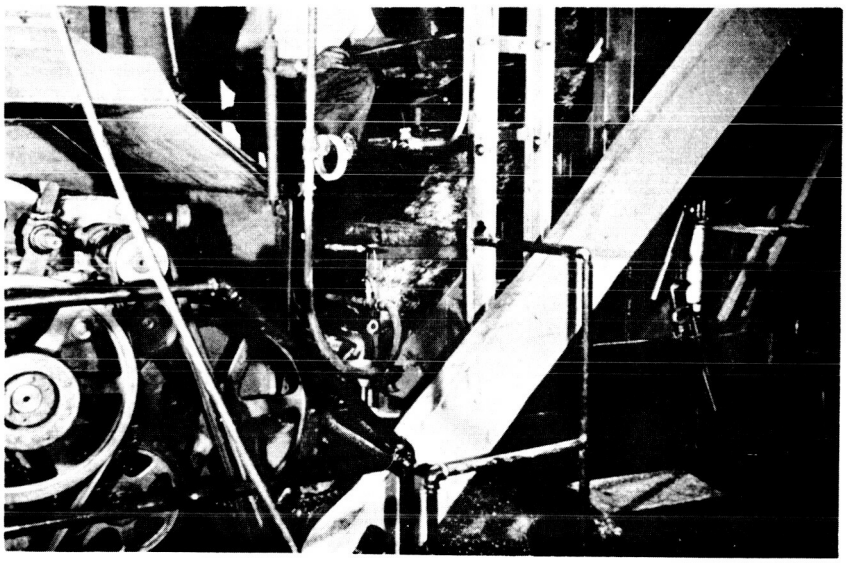

FIGURE NO. 28 GARNETT OPERATION

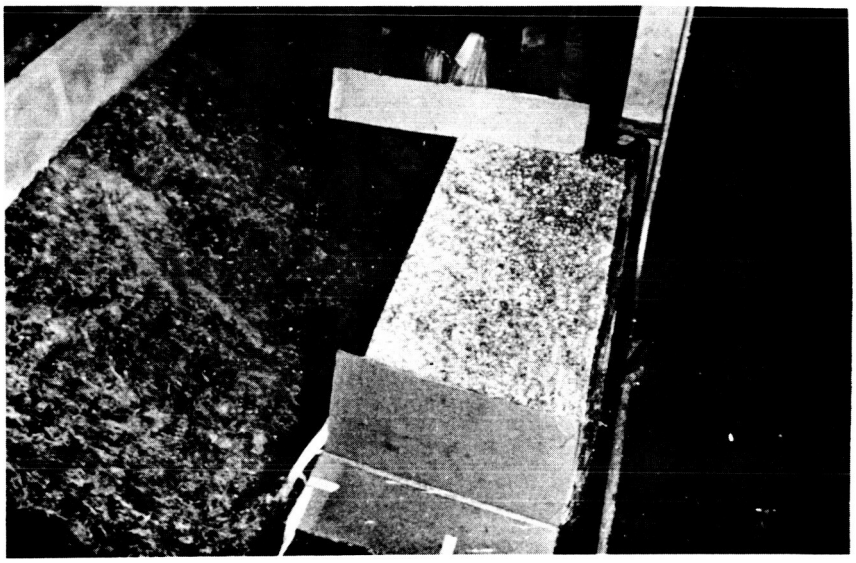

FIGURE NO. 29 BLENDED VEIL

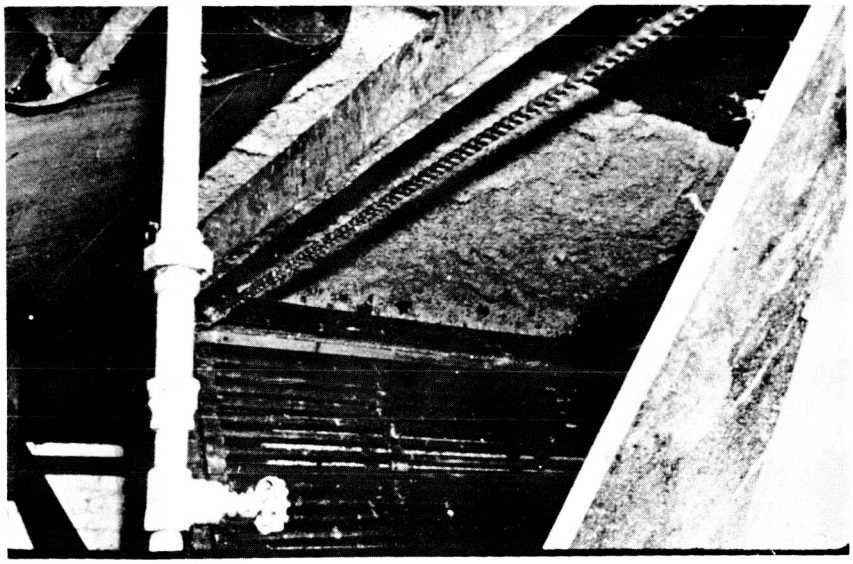

IGURE NO. 30 CROSSING & WETTING OPERATION

FIGURE NO. 28 GARNETT OPERATION

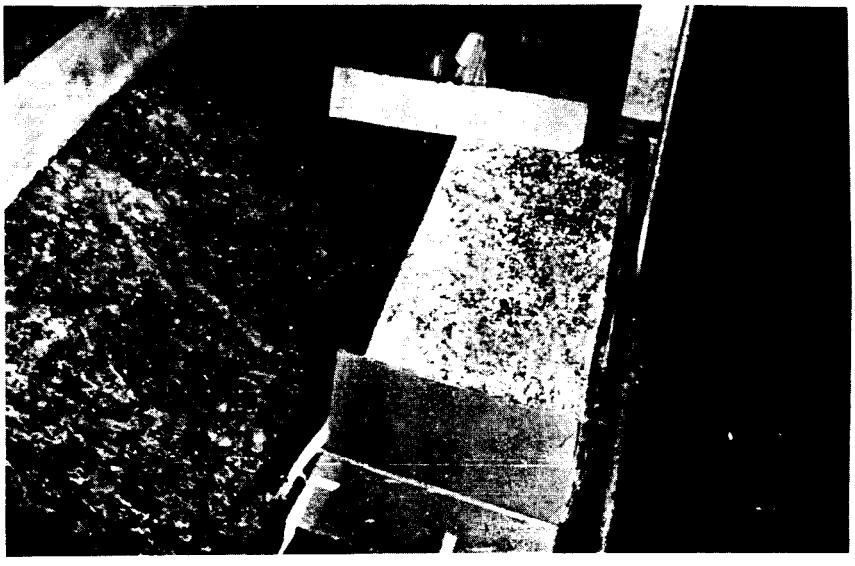

FIGURE NO. 29 BLENDED VEIL

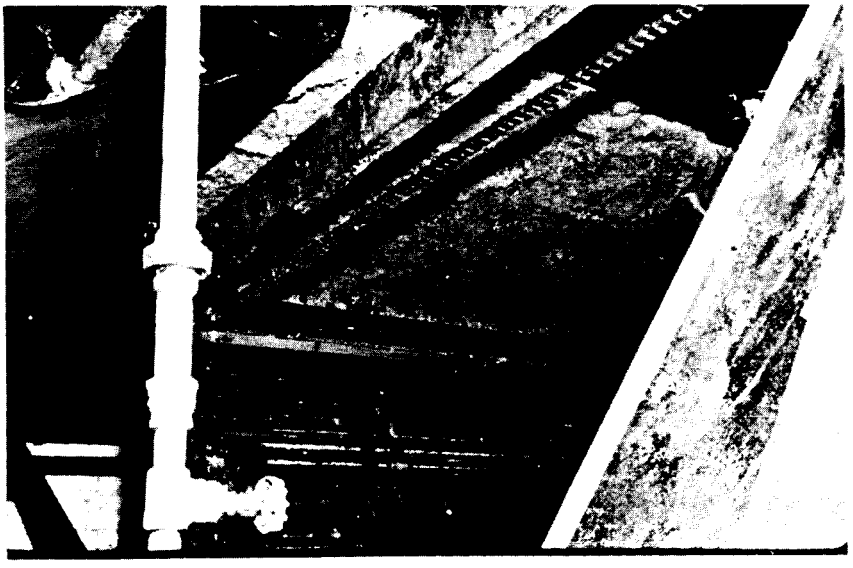

IGURE NO. 30 CROSSING & WETTING OPERATION

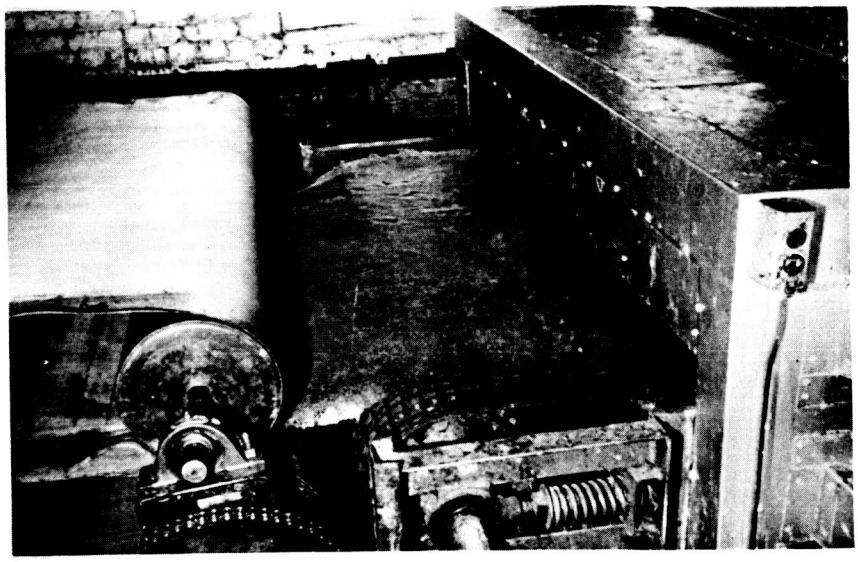

FIGURE NO. 31 WET LAP

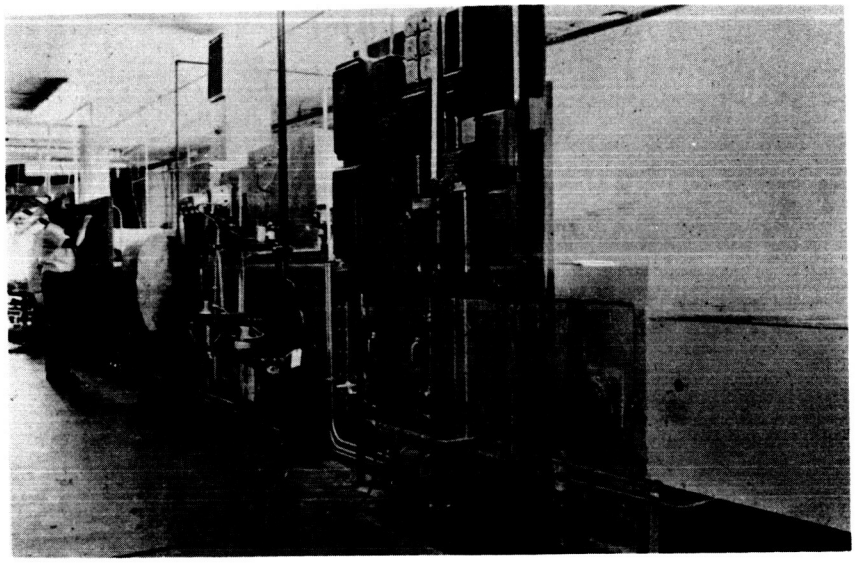

FIGURE NO. 32 CURING OVEN

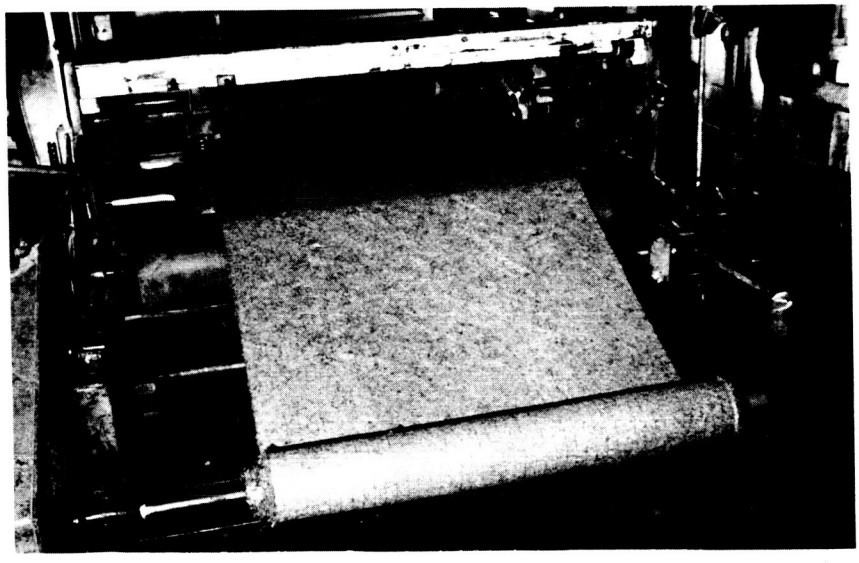

FIGURE NO. 33 FINISHED COMPOSITE MAT

RANDO-FEEDER AND RANDO-WEBBER FIBROUS WEB SYSTEM

The equipment which was used for these blending operations is based upon a commercial method of air-laying fibrous webs by using what is known as the Rando-Feeder and Rando-Webber machines. These machines were made by the Curlator Corporation, East Rochester, N. Y. A few trial runs on this equipment at J. P. Stevens Company Central Research Laboratories in Garfield, N. J., indicated that this machinery was much better suited for the webbing or matting operations involving the fibers selected for this program. This machinery allowed mat formation which essentially overcame the problems encountered with the use of the Proctor machinery previously employed.

The functioning of this processing equipment can best be described by referring to the sketch in Figure No. 34 and following the flow of the materials through the Rando-Feeder and Rando-Webber equipment. The fibers in their dry form were placed in the hopper and thereby entered the system comprised of the two machines operating as a unit. The primary function of this feeder portion was to produce a uniform mat in tuft form. The creeping delivery apron (17) introduced the fibers to the elevating apron (2) with its slats and pins which picked up the fibers from the creeping delivery apron and raised the tufts of the fibers to the stripper apron (3). At this point the excess fiber was removed by the stripper apron and returned to the hopper. The small tufts of fibers remaining on the pins passed over the top of the apron into the region known as the airbridge (4).

This unique airflow device accomplished the doffing of the required amount of fiber by means of the air stream over the pins into the airbridge. The amount of material conveyed is proportional to the flow rate of the air employed. If any foreign medium, such as tramp metal, wood, or even coagulated fiber clumps, are included in the initial operations, they are dropped out and collected in the trash chamber (8) at the bottom of the elevating apron. Since air is the carrying medium, these heavier materials fall out.

The flow rate is governed by the speed of continuous formation on the feed mat condenser screen (5). Since the air pressure above the screen is below atmospheric, air must flow through the screen into the suction duct as indicated by the arrows. When the operation of the screen is just starting and there is no mat formation on the screen, a maximum quantity of air flows through the screen both from the airbridge and between the rolls of the roller conveyor (6).

This condition caused doffing to occur at a maximum rate and the fibers to be deposited in a wedge opening between the screen and the conveyor rolls. As the mat structure takes shape the air flow is reduced by the resistance of the mat on the screen and on the throat of the airbridge. Proportionately less doffing occurs until a condition of equilibrium is reached. At this point sufficient fibers have been doffed to form a continuous uniform mat.

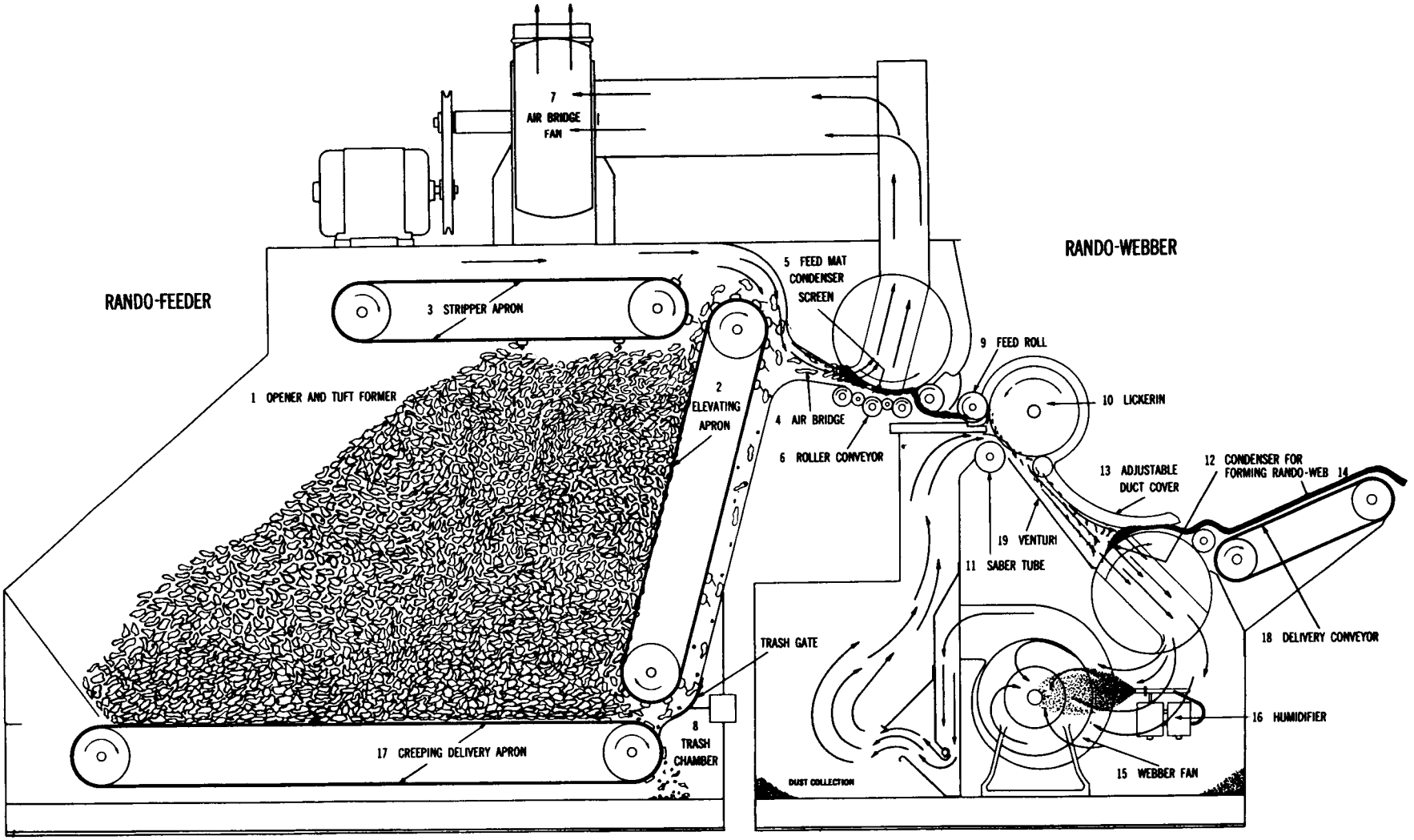

FIGURE NO. 34 SCHEMATIC FLOW DIAGRAM COMBINED RANDO-FEEDER

& RANDO-WEBBER

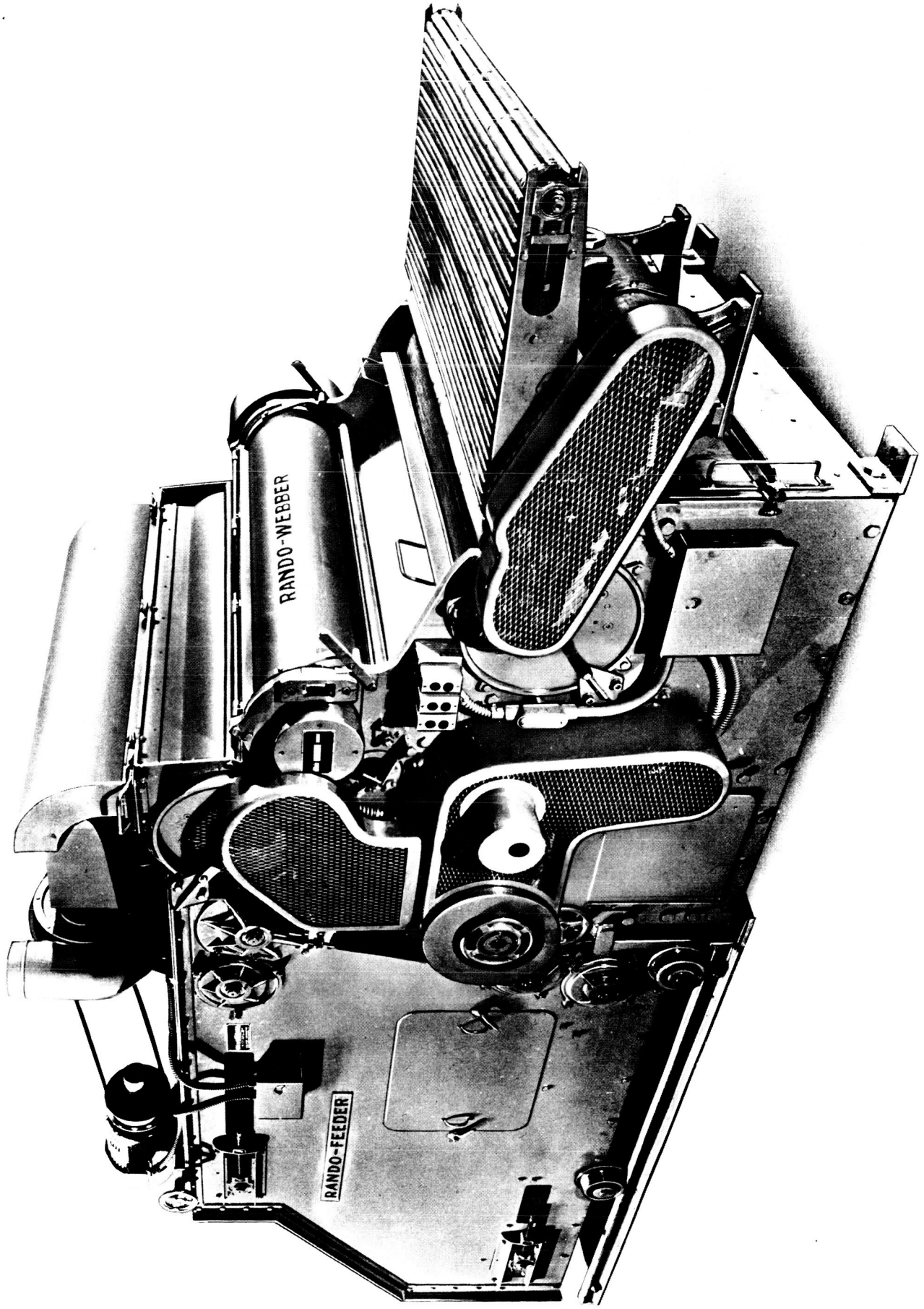

FIGURE NO. 35 RANDO-FEEDER & RANDO-WEBBER

Any excess stock which has not been carried across the airbridge is returned by the pins to the bottom of the feeder for reuse. An overload condition can not exist because when the mat builds up to a point where sufficient resistance is offered to the air flow doffing of the fiber from the apron pins is prevented. The opened material then continues to travel around the elevating apron allowing operation to continue in this condition indefinitely. The feed mat condenser drive is synchronized with the Webber equipment. The ability of the airbridge to make a constant and practically instantaneous equalization, both lengthwise and crosswise as the fiber material is presented to the screen wedge, insures a uniform feed mat.

From this Rando-Feeder the fiber mat entered the Rando-Webber under the feed roll (9) and was fed by this roll into the concave surface formed by the nose bar. Compression occurred here as the fiber mat was fed under the top of the nose bar into the path of the teeth on the lickerin cylinder (10) which removed individual fibers from the mat on the tips of its teeth. The fiber was then carried by the teeth to the high velocity air stream formed by the throat of the venturi shaped duct (19). At this point the fibers were swept from the teeth by the air stream on the downstream side of the lickerin. The material in fibrous form was again airborn and subsequently deposited on the condenser to form a Rando-Web (14). By allowing the air to pass through the circular screen into the closed duct system, the fibers were laid at random on the revolving condenser screen. The result was a continuous random web flowing from the condenser screen to the delivery conveyor (18).

This unique design of the Rando-Feeder and Rando-Webber equipment permitted an efficient production of high quality rendom webs in which there was little or no fiber loss. This equipment and system of forming mats greatly enhanced the degree of control of these fibers and applied the exact science of web formation required for a program of this type, since many of the important physical properties of the end product are dependent on whether the fibers are oriented or deposited at random.

APPENDIX 2

TESTING PROCEDURES AND EQUIPMENT

SPECIFIC HEAT DETERMINATION

This method for determining specific heats of thermal insulating materials follows closely to the method suggested in ASTM Designation: C-351-61. The only deviation from ASTM is in the instrumentation techniques.

The principle of this method consists essentially of adding a known mass of material at a known high temperature to a known mass of water at a known low temperature and determining the equilibrium temperature that results. The heat absorbed by the water and the containing vessel was calculated and this value equated to the expression for the heat given up by the hot material. From this equation the unknown specific heat was calculated.

Apparatus

1. Calorimeter - an unlagged 500 ml Dewar flask.
2. Magnetic stirrer with speed-regulating device.
3. Heater - cylindrical open-end radiation type.
4. Capsule - a hollow brass cylinder approximately 1 inch in diameter by 2 inches in length. A thermocouple well mounted into the re= movable cap extends into the cavity.
5. Specimen thermocouple - No. 30 B&S gage iron-constantan wire monitored on a Minneapolis Honeywell Model 2714 laboratory potentiometer with compensating reference junction.
6. Five junction differential thermopile - No. 30 B&S gage copper-constantan wire for sensing water differential temperature. The resulting emf is recorded on a Leeds & Northrup Speedomax G single line recorder.

Calibration

The water equivalent of the calorimeter and its accessories must be determined. This is the mass of water that requires the same amount of heat as the given body to raise its temperature by an equal amount. In formulation this is designated by E.

The next step is to determine the thermal capacity of the capsule. This is the energy added to the water by the heated capsule. In formulation this is designated by McCc.

The final calibration step is to check the specific heat of a known specific heat standard. Electrolytic copper is used for this check.

PROCEDURES

The specimen or specific heat standard was placed into the capsule with the measuring thermocouple in place. It was then lifted into the vertical heater by means of a non-absorbing thread. When the capsule and specimen were in thermal equilibrium in the heater they were dropped into the Dewar flask containing a known mass of water. The temperature rise of the water was then sensed by the differential thermopile and recorded on the strip chart recorder. When the slope of the temperature vs. time curve was constant for a period of ten minutes the test was terminated. A straight line was then drawn tangent to the slope back to time zero intercept. Utilizing this method the thermal exchange that took place at time zero was considered instantaneous and was proportional to the temperature difference.

Formulation

$$E = \frac{Mr\,Cr}{Cw}\,\frac{(Th-Tm)}{(Tm-Tc)} - Mw$$

$$McCc = \frac{(Mw + E)\;\; Cw\;\; (Tm-Tc)}{(Th - Tm)}$$

$$Cs = \frac{\dfrac{(Mw + E)\;\; Cw\;\; (Tm - Tc)}{(Th - Tm)} - McCc}{Ms}$$

Symbols ----- The symbols used in the equations have the following significance:

E =Water equivalent of the calorimeter and its accessories, in grams.
Mr =Mass of the specific heat standard, in grams.
Cr =Mean specific heat of the specific heat standard over the range Th to Tm, cal. per gm, per deg, Cent. (=0.0931 for copper over the range 100 to 20C).
Th =Temperature of the capsule and specimen, capsule, or standard after heating, deg. C.
Tm =Temperature of the mixture extrapolated back to time zero, deg. C.
Cw =Mean specific heat of calorimeter water, cal. per gm. per deg. Cent.
Tc =Temperature of the calorimeter water before capsule and specimen is dropped, deg. C.
McCc=Thermal capacity of the capsule assembly, cal. per deg. Cent.
Mw -Mass of calorimeter water, in grams.
Ms -Mass of specimen, in grams.
Cs =Mean specific heat of test specimen over the temperature range Th to Tm, cal. per gram per deg. Cent.

Figure 36 depicts the recorded data for a typical specific heat determination (composite material No. 1A, the second test determination of a series of three).

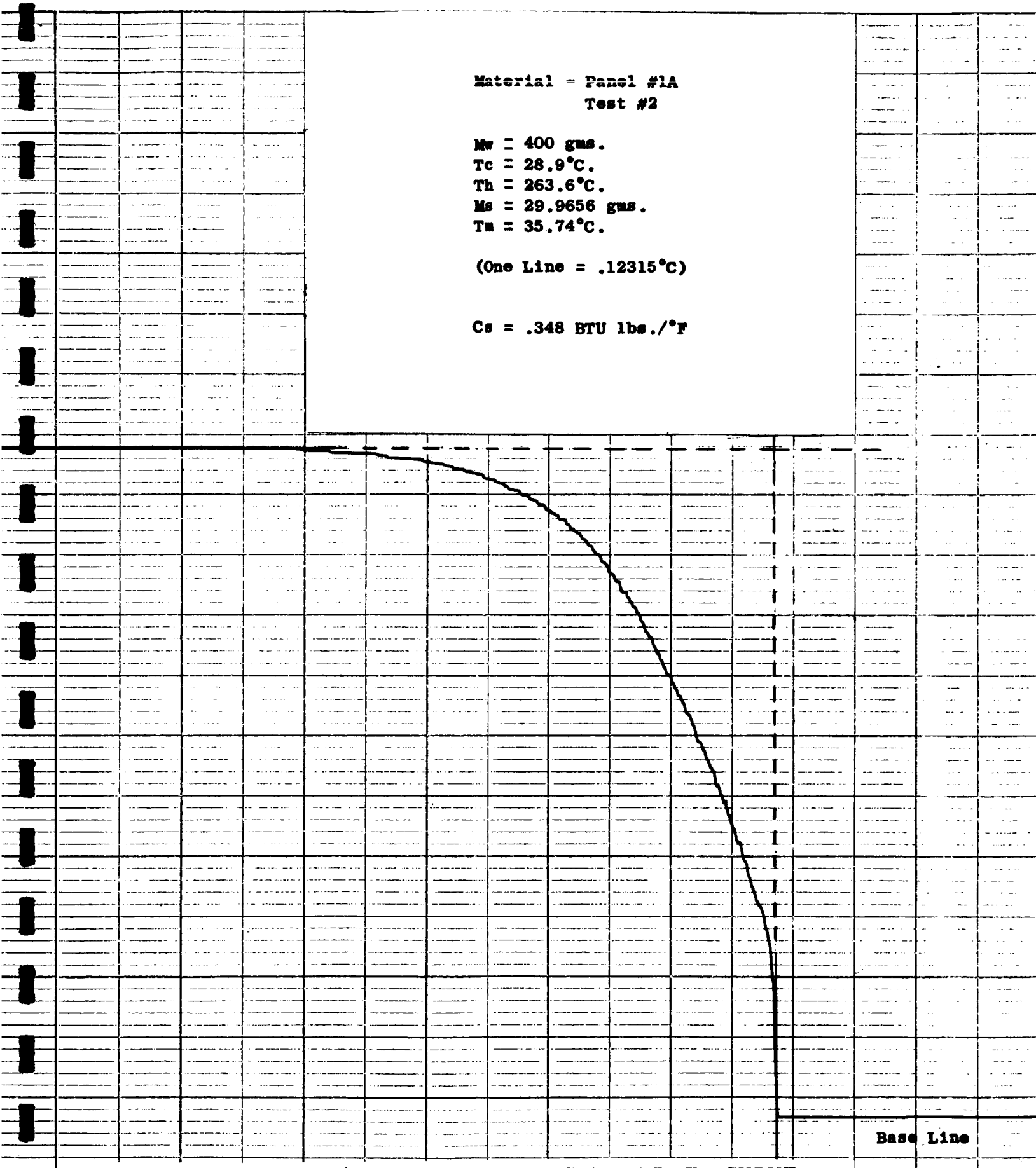

FIGURE NO. 36 TYPICAL SPECIFIC HEAT DATA CURVE

THERMAL CONDUCTIVITY DETERMINATION

This procedure for determining the thermal conductivity of insulating materials conforms to the ASTM guarded hot plate method, designated as ASTM C177-45.

Basically this method consists of heating one side of a slab or plate to a known high temperature while maintaining the opposite side at a known low temperature and measuring the rate of heat flow, under steady conditions, through a unit of area, per unit of temperature gradient in the direction perpendicular to the area.

Apparatus

1. The hot plate consists of an Alundum plate 3/8" thick and 9" in diameter. The heating elements are No. 20-24 (AWG) Nichrome V resistance wire.
2. The temperature sensing elements consists of eight chromel-alumel P thermocouples cemented in the two faces of the plate (4 in each) diametrically opposite each other. The couples are placed at a distance 1-7/8", 2-5/8", 3-3/8", and 4-1/8" respectively from the center of the plate.
3. Two bronze cooling plates 9" diameter and 1" thick with inside dimensions of 8-1/2" x 1/2" are used to maintain the low temperature on the specimen.
4. The completed apparatus is assembled in a circular container of asbestos lumber 22" diameter and 10" in height.
5. Mica pellets are used to cover the completed apparatus to minimize guard heater edge losses and effect of room ambient temperature changes.
6. Two Wheelco Model 402 Capacitrols with a range of 0-1000°F. regulate the temperature of the center and guard heaters.
7. A Temprite Model R-24W cooling bath is used to regulate and cool the cold plates.
8. Two Cramer timers are used for determining average power input.
9. Triplet voltmeters and ammeters are used for determining wattage-input.
10. An L&N Model K-3 universal potentiometer is employed as the temperature indicating device.

Procedures

One each of two specimens of the test material 9 inches in diameter and up to 1 inch thick was placed between the Alundum hot plate and one of the cold plates, sandwich fashion.

The plate assembly was then covered with the mica pellets.

Controller's indices were moved to set points to provide for desired hot-to-cold plates temperature differential and equal guard and central heater temperatures.

Console was activated.

After set temperatures were attained and thermal steady-state condisions were established, timers were switched on.

Voltmeter and ammeter reading was noted.

Timers were switched off after required timing interval had elapsed (usually 30 minutes is sufficient.).

Formulation

$$K = \frac{W \times C \times L}{H \times A}$$ where:

K = Thermal conductivity expressed as B.T.U. in/ft^{2}hr. ^{o}F.
W = Wattage input: determined by multiplying the voltage by the amperage and multiplying this by the ratio of heater on time to total elapsed time.
C = Factor for conversion of wattage into B.T.U. /hr. (3.414)
L = Length of path of heat flow (average thickness of two specimens.).
H Temperature of hot plate minus temperature of cold plate.
A = Actual area normal to the path of heat flow (flat surface).

Thermal conductivity determinations were not performed on the individual fibrous reinforcements.

SPECIFIC GRAVITY AND DENSITY DETERMINATIONS

Verification of handbook data and testing of the virgin, fibrous materials was performed by employing a Beckman Model 930 air comparison pycnometer.

Specific gravity and density of the molded test panels was performed in complete accordance with the ASTM D792-60T methods and also with the air comparison pycnometer.

MELTING POINT DETERMINATIONS

Method 1

The melting point determinations were originally to be made by using an arc image furnace. However, such equipment was not available at the time the tests were to be performed and the determination method was changed to the standard ASTM C24-49 procedure. This method called P.C.E. or Pyrometric Cone Equivalent was one in which the material was made into cones of a specified length and heated at a definite rate. The temperatures at which

The points of the cones touched their bases were recorded as their melting points.

All virgin, fibrous materials and test panels were subjected to this procedure (described in detail in a booklet published as the 4th Edition, in June 1961, by Orton Memorial Laboratory of Columbus, Ohio entitled "The Properties and uses of Pyrometric Cones"). The one exception being the graphite fibers and the primarily graphite fiber test panels. Handbook data was employed for these fibers and melting points of the test panels were not determined.

Since these materials, like most other common substances, did not actually have a melting point or a fusion temperature but rather fused over a range of temperatures, it was decided to employ a different method for future determinations.

Method 2

This method was to employ motion pictures, as a visual indication of the mass degradation of each specimen tested on the Arc Plasma Generator (APG), to determine the exact time of degradation or mass melting. This was then related to the time-temperature history plotted for each test run to determine the mass degradation or mass melting temperature. The mass degradation or melting point was considered as that time when visually the composite appeared to have a wave-like molten mass flow across its whole surface, not just individually isolated melting of the lowest melt temperature fibrous constituent. These values were cross correlated with the melting point values previously determined on the composites by the standard Pyrometric Cone Equivalent methods. The standard methods indicated that the composites degraded in stages and did not act as eutectics or as homogeneous mixtures normally act.

MASS LOSS RATE DETERMINATION

Mass loss rate determinations were made from measurements of the dimension and weight changes of 4" x 1" x 1/2" APG test specimens, cut from the molded composite test panels, when they were exposed to preselected conditions of the APG.

EMISSIVITY DETERMINATION

Emissivity determinations were made during the APG test runs using the APG as the heat source. Instrumentation employed for this determination included a total radiation pyrometer, calibrated against a black body, supplemented by an optical pyrometer. Complete description of the instrumentation employed is contained in later paragraphs.

EFFECTIVE THERMAL CONDUCTIVITY DETERMINATION (above the sublimation or melting point of the specimen)

The heat source for these determinations was the APG. Data was derived from the relationship between temperature and time at the preselected constant cold wall heating rates by employing the calculation method detailed on the data tables. The instrumentation of the test specimens is also indicated on the data table listings included elsewhere in this report. The time-temperature recording instrumentation employed is discussed in later paragraphs.

EFFECTIVE HEAT OF ABLATION

The determination of the effective heat of ablation was made using the APG as the heat source. The data generated was based on the relationship between the hot wall heating rate and the mass loss rate of the test specimen.

ARC PLASMA GENERATOR (APG) DESCRIPTION

GENERAL OPERATING PARAMETERS

CTL's 1.5 megawatt arc plasma generator can be operated using air, nitrogen, and/or oxygen at gas mass flow rates ranging from 0.008 lb./sec. to 0.25 lb/sec. over a wide range of chamber pressures including sub-atmospheric to 35 atmospheres. It also can be operated on such gases as ammonia, argon, carbon dioxide, helium or hydrogen.

Heat flux and enthalpy rates can be varied as required by varying input power and gas flow to the generator. Various sub-sonic nozzles are available which will operate at enthalpy conditions from 1500 to 7,000 BTU/lb and at stagnation pressures from atmospheric up to 500 psia.

A nominal Mach 3 nozzle is available for supersonic plasma flow testing. This nozzle has a throat diameter of 1.086 in. and an exit diameter of 2.91 inches. When operated in conjunction with the vacuum system, a gas velocity equivalent to Mach 3.56 can be obtained.

The vacuum test chamber, 53 in. dia. x 8 ft. length, is equipped with a test bed for mounting and positioning test specimens at the nozzle discharge. A 5 stage steam ejector system provides vacuum capability down to 0.050 mm. Hg (230,000 ft. altitude) at no-flow conditions.

By utilization of various nozzles and shrouds, it is possible to accomodate 3" maximum diameter test specimens for splash testing and 2" maximum diameter specimens for shroud testing. A water-cooled, rectangular test tunnel, 1" x 0.22 in. cross section, adapted to a 1 inch diameter sub-sonic nozzle will provide and measure cold wall heat flux rates up to 700 BTU/sq. ft. sec., utilizing rectangular, flat plate test specimens 1" x 3". Shear forces up to 20 lbs/sq. ft. can be obtained with this tunnel test section.

The instrumentation employed records all test data on individual readouts as well as central recording on Honeywell Model 1612 visicorder oscillograph. Due to its rapid response, this instrument is especially suited for recording arc facility and specimen environmental conditions during transient-type testing. Temperature histories through the specimens, shear resistance through various velocities, ablation rates (linear and mass loss), as well as the heat of ablation of specific materials can be established.

GENERAL DESCRIPTION

The CTL solenoid arc-plasma generator (APG) produces high-enthalpy gas flows by the energy exchange from a rapidly moving direct-current arc confined in an annulus formed by concentric water-cooled electrodes. Arc motion is derived from the force vector resulting from the mutual interaction of essentially perpendicular flux fields. The arc column resulting from the high intensity, direct-current flow within an ionized path is driven with sufficient velocity such that the arc-terminal residence times are extremely short, preventing electrode surface melting and ablation. The high-intensity flux field necessary to produce arc motion is derived from direct-current excitation of a solenoid coil enclosing the arc chamber. The electrodes and exposed elements of the arc chamber are water-cooled to absorb the large amounts of thermal energy transmitted to and conducted through the surface.

The unit consists of a water-cooled arc chamber whose surface acts as the cathode - or electron-emitter element of the electrical circuit. The positive (anode) element is mounted concentric with the cathode shell and oriented near the plane of symmetry of the flux field generated by the water-cooled coil surrounding the assembly. Provision for gas injection is contained on the water-cooled back plate and suitable nozzles can be mounted in the arc-chamber exit plane to channel and accelerate the exhausting plasma for test application.

The APG is arranged so that gas can be injected through a secondary system downstream of the arc zone. This permits testing with highly oxidizing atmospheres which might be harmful to the electrodes in the arc zone. The secondary gas is injected in a manner which provides adequate mixing of the primary and secondary gas flows, resulting in a homogeneous mixture when expanded through a nozzle or other orifice attached to the APG. The secondary gas-injection ring operates at cathode potential and is held in place by a mating nozzle.

Arc operation is presently accomplished by ionizing the gases in the immediate region of the cathode bump by a shorting-wire explosion or high-frequency arc discharge. Current flow between the electrodes maintains a high degree of ionization of the oncoming gas such that continuous arc operation ensues. Current and voltage characteristics are varied by combinations of electrode spacing, power supply and ballast resistance settings, chamber pressure and gas flow rate, and the type of fluid being used as the test medium.

FIGURE NO. 37 APG TEST FACILITY

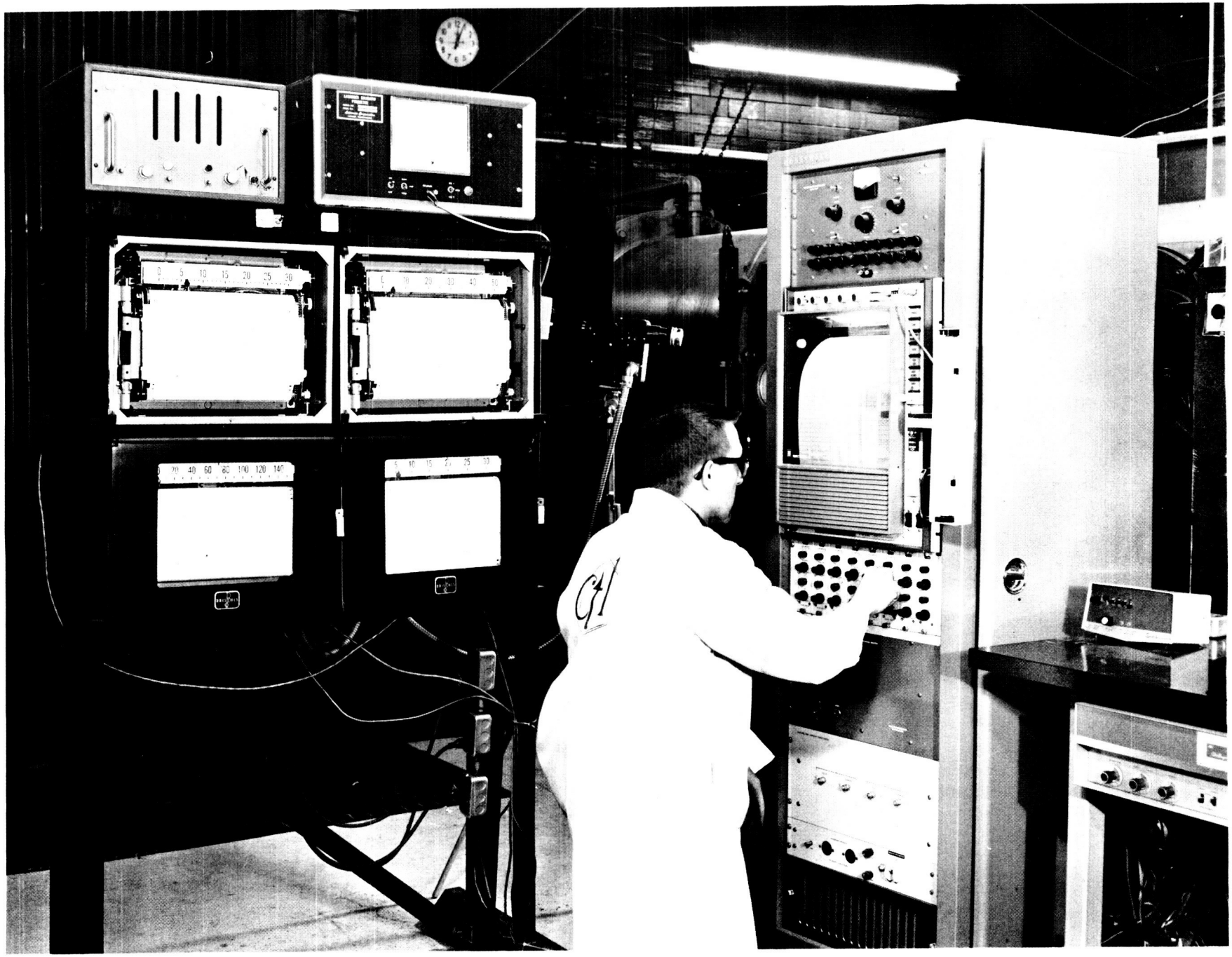

FIGURE NO. 38 RECORDING INSTRUMENTATION

RECORDING OSCILLOGRAPH

The instrumentation employed records all pressure, temperature, and electrical test data on individual readouts as well as central recordings on a Honeywell Model 1612 Visicorder Oscillograph.

This unit employs a high-pressure mercury lamp with maximum output in the ultra-violet region. Signals from external sources are fed into sub-miniature galvanometers and are transferred into moving beams of light by the galvanometer mirrors. The light reflected by the mirrors is transmitted through a precision optical system and focused directly onto the recording paper, which is highly sensitive to ultra-violet light.

The total system is rack-mounted and has 36 channels, each of which is capable of recording static or dynamic data at frequencies from D.C. to 5000 cycles per second on 12 inch paper. 20 galvanometers are employed. 9 of the M40-350A type are used for temperature recording and 7 of the M100-350 type are used for voltage and 2 each for the current recordings. The galvanometers may be deflected as much as 8 inches peak to peak and maintain specified linearity. The amplitude linearity is within 2% of the indicated reading over the galvanometer's full scale deflection.

The Model 1612 has 15 forward speeds, which permits review, study, and notations to be made while testing is in progress.

The remainder of the unit is comprised of an 8 module rack adapter with 8 pressure gage control units; and 18 channel thermocouple calibration and temperature compensation unit; and the attendant instrumentation rack, pressure transducers, and voltage and current attenuation control panels.

PYROMETERS

Two types of pyrometers are used for sensing specimen surface temperature. The first type is the Leeds - Northrup Total Radiation Pyrometer, Type 8861. The two small target, high speed Rayotube radiation sensors provide the following temperature ranges.

(1) 1850 - 4000°F.
(2) 3000 - 7000°F.

Target diameter of the Rayotubes at 12" focus is 0.26". Output from the Rayotubes is recorded on a Visicorder oscillograph, providing excellent coordination with other recorded data from the Arc Plasma Generator and the test specimens.

Satisfactory solutions for many temperature measuring problems are not accomplished, however, by the standard optical pyrometer or total

radiation pyrometer. This is primarily because the emissivity factor of the specimen surface must be known at the temperature for accurate high temperature measurements.

The second type of pyrometer available, a Latronics Coloratio Pyrometer, Model BF 222 eliminates the emissivity factor since its basis of operation is independent of total radiation. This pyrometer measures temperature by measuring the relative intensities of two color bands (red and blue) of the visible spectrum being emitted and then determining the ratio of these two intensities, which is directly proportional to the temperature of the emitting surface.

The pyrometer has a total temperature range of 2500 to 7500°F. over the following range bands:

(1) 2500 - 4500°F.
(2) 4000 - 6000°F.
(3) 6000 - 7500°F.

The temperature is indicated on a precision meter, calibrated directly in degrees Fahrenheit, with a linear scale. A millivolt output is also recorded on the Visicorder oscillograph, for coordination with the other recorded data from the test facility. Response speed of the Coloratio pyrometer can be as fast as 0.2 seconds, or as slow as desired.

Figure Nos. 37 and 38 disclose the APG arc head and portions of the recording instrumentation which is employed.

APPENDIX 3

ANALYTICAL PROCEDURE FOR THE WEIGHT PERCENTAGE DETERMINATION OF THE FIBROUS AND RESINOUS CONSTITUENTS OF COMPOSITE TEST PANELS

SUMMARY

Utilizing the method for B_2O_3 determination in glass; sample weights after 325°F. for 20 min., 950°F. for 4 hours, and 1200°F. for 16 hours; and data on weight losses of graphite, glass, and asbestos fibers used in the composites after exposures to the same temperatures and for the same times listed above, calculations are made on the % composition of each constituent. Factors calculated are % glass, % asbestos, % graphite, and % resin.

DISCUSSION

Being quite similar in composition, the glass and asbestos fibers proved the complicating factor in this determination. However, the nominal composition of the glass and asbestos (Table A) shows some differences.

TABLE A

Constituent	"E" Glass %	Asbestos %
SiO_2	50-52	38-40
MgO	0-6	40-44
Al_2O_3	12-16	0.1-4.0
CaO	16-25	0-0.15
B_2O_3	7-13	-----
Na + K Oxides	1-4	-----
Fe_2O_3	----	0.4-3.0
FeO	----	0.2-2.0

Samples of the raw glass fibers used in the mats must be analyzed for B_2O_3 content as a basis for glass determination.

Boric oxide (B_2O_3) was selected as the identifying material for two reasons:

(1) The "E" glass is a manufactured product and has the most uniform composition.

(2) The B_2O_3 is present only in the glass and is present in a significant amount.

PROCEDURE

This analytical procedure is performed as indicated by the attached flow sheet and is described in the following paragraphs:

FLOW SHEET (Used in conjunction with Table B)

I (wgt.)

Sample:

1. Glass & sizing
2. Asbestos & Volatiles
3. Graphite
4. Resin volatiles & solids

Subjected to 325°F. for 20 minutes

↓

II (wgt.)

1. Resin volatiles ↗
2. Resin solids and all other constituents of sample

Subjected to 950°F. for 4 hours.

↓

III (wgt.)

1. Resin solids burn-off plus glass, ↗ asbestos & graphite losses.
2. Graphite, glass, asbestos

Subjected to 1200°F. for 16 hours

↓

IV (wgt.)

1. Graphite burn-off plus ↗ asbestos & glass losses
2. Graphite ash which is neglected (.2%) ↗
3. Glass, asbestos

Subjected to $B_2 O_3$ Determination

↓

1. Glass (by boron analysis), asbestos (by difference) and back calculate for other constituents as shown for composite determination.

A representative sample (A) of 4-6 gms. of mat or laminate is cut or pulverized as finely as possible. It is then weighed and the weight recorded. The sample is heated for 20 min. at 325°F and again the weight is taken and recorded. The sample is further heated at 950°F for 4 hours, weighed, and recorded. Next, it is heated for 16 hours at 1200°F, weighed and recorded. A final determination can now be made on the boron content as described in the attached procedure taking an appropriate sample (B). Calculations can be made as follows, neglecting graphite ash:

(1) Glass in (B) after 1200°F = $\text{gms.} \frac{B_2\,0_3}{\%\ B_2\,0_3 \text{ in glass}} \times 100$

(2) Glass in (A) after 1200°F = $\frac{\text{(A) wgt. total sample}}{\text{(B) wgt. total sample}} \times \text{glass in (B)}$

(3) Asbestos in (A) = total wgt. (A) - glass in (A).

(4) Calculations are made on weight losses due to glass and asbestos after heating at 950° and 1200°F. using Table B. There is no loss of weight by the fibers at 325°F due to the resin coating.

TABLE B

	% Wgt. loss	
Substance	325–950°F	950–1200°F
Asbestos	2.8	11.2
Glass	.88	.50
Graphite	3.05	96.95 *

Total wgt. loss for glass = 1.38%.

*Residual .2% graphite ash is neglected.

For example, if 1 gm of glass were determined to be present after 1200°F., then initially there was $\frac{1 \text{ gm. glass}}{100\% - 1.38\%} \times 100 = X$ gms. of glass. At 950°F. the loss was .99% (X gms.) etc..

(5) Thus the weight loss after heating at 1200°F. was composed of glass and asbestos losses as well as graphite burn-off. Graphite at 950°F was then determined.

Sample wgt. (A) 950°F. - Sample wgt. (A) 1200°F. = total wgt. loss 950° to 1200°F. Graphite at 950°F. = total loss - asbestos loss - glass loss.

(6) Determinations for graphite were made as described in (4).

(7) The weight loss from 325°F. to 950°F. was due to volatiles from the asbestos, sizing from the glass, and oxidation of the graphite as well as the burn-off of resin solids. Therefore, resin solids was calculated:

Resin Solids = Loss in sample wgt. (A) 325° to 950°F. - Asbestos loss - Glass loss - Graphite loss.

(8) The weight loss from initial to 325°F. was due to resin volatiles.

Procedure for determining amount of boron in glass

This method makes use of an organo-metallic complex of boric acid for the determination of B_2O_3 in glass. The amount of the acid present is determined titrimetrically with sodium hydroxide. The procedure as described below is routinely accurate to within .15% of the actual B_2O_3 content.

A sample is cut or pulverized as finely as possible and mixed with 6 times its weight of sodium carbonate. The mixture is fused over a blast burner until a homogeneous melt is achieved. The melt is allowed to cool to room temperature, re-exposed to the burner momentarily to free it from the crucible and cooled again. The melt is dissolved in a 250 ml. Erlenmeyer flask using 50 ml. of 1:1 hydrochloric acid. The solution is neutralized with calcium carbonate adding about 1 gm excess, refluxed for 15 minutes and filtered through Whatman #40 filter paper or equivalent into a 500 ml. evacuating flask. It is acidified to methyl red indicator, heated to 80° C., subjected to a vacuum of 25 inches of mercury to remove residual CO_2, and cooled to room temperature. .05 N sodium hydroxide is used to titrate to a pH of 5.4 25 grams of mannitol are added and the solution is titrated to a pH of 6.8 taking note of the Na OH used after mannitol addition. Calculations are made as follows:

$$N_{NaOH} \times V_{NaOH} = \#\text{ moles B}$$

$$\#\text{ moles } B_2O_3 = \frac{\#\text{ moles B}}{2}$$

$$g\ B_2O_3 = 69.64\ (\#\text{moles } B_2O_3)$$

$$\%\ B_2O_3 = \frac{g\ B_2O_3}{\text{sample wgt.}} \times 100$$

A similar procedure is applicable for the determination of a sample containing asbestos and graphite ash in addition to glass.

Sample Calculation - Mat 1B

Weights: I - 4.7331 = Sample (A) % B_2O_3 in glass = 7.0%
II - 4.2826 = Sample (A)
III - 2.4540 = Sample (A)
IV - 2.1023 = Sample (A)
Sample (B) = 0.6788

moles B = $N_{NaOH} \times V_{NaOH}$

= .05093 (.00235) = .0001197

moles B_2O_3 = $\frac{\text{\# moles B}}{2}$ = $\frac{.0001197}{2}$ = .0000599

g B_2O_3 = 69.64 (.0000599) = .004178

(1) Glass in (B) after 1200°F. = $\frac{\text{g } B_2O_3}{\%\ B_2O_3 \text{ in glass}} \times 100 = \frac{.004178}{.0704} = .05938$

(2) Glass in (A) after 1200°F. = $\frac{\text{(A) wgt. total sample}}{\text{(B) wgt. total sample}} \times$ glass in (B)

$= \frac{(2.1023)}{.6788} \times .05938 = .1839$

(3) Asbestos in (A) = total wgt. (A) - Glass in (A)
= 2.1023 - .1839
= 1.9184

(4) Asbestos and glass wgt. losses:

wgt. losses: initial glass = $\frac{.1839}{100\%-1.38\%} = \frac{\text{Glass}}{.1864}$ Asbestos

initial asbestos $\frac{1.9184}{100\%-14\%} = 2.2307$

950°F.	.0016	.0625
1200°F.	.0009	.2498

(5) Graphite at 950°F. = sample A 950°F. 2.4540
sample A 1200°F. 2.1023
loss .3517
- glass .0009
- Asbestos .2498
graphite = .1010

(6) Graphite wgt. losses
total graphite = $\frac{.1010}{.9695} = .1042$
loss 950 = .0032
loss 1200 = .1010

(7) Resin solids:

sample A 325°F.	4.2826
sample A 950°F.	2.4540
loss	1.8286
- glass	.0016
- asbestos	.0625
- graphite	.0032
resin solids	1.7613

(8) Resin volatiles:

sample A init.	4.7331
sample A 325°F.	4.2826
	.4505

% Composition: *

$$\% \text{ glass} = \frac{.1864}{4.7331} \times 100 = 3.938\%$$

$$\% \text{ asbestos} = \frac{2.2307}{4.7331} \times 100 = 47.13\%$$

$$\% \text{ graphite} = \frac{.1042}{4.7331} \times 100 = 2.202\%$$

$$\% \text{ solids} = \frac{1.761}{4.7331} \times 100 - 37.50\%$$

$$\% \text{ volatiles} = \frac{.4505}{4.7331} \times 100 = 9.229\%$$

$$\% \text{ resin} = \% \text{ solids} + \% \text{ volatiles} = 37.50 + 9.229 = 46.73\%$$

*Final composition used for charting purposes is given on basis of three determinations. Above values are for one determination only.